Preliminary observations on the geology of the southern Big Salmon Range, south-central Yukon (parts of NTS 105C/13, 14, 105F/4 and 105E/1)

D. Moynihan*
Yukon Geological Survey

J.L. Crowley
Boise State University

Moynihan, D. and Crowley, J.L., 2022. Preliminary observations on the geology of the southern Big Salmon Range, south-central Yukon (parts of NTS 105C/13, 14, 105F/4 and 105E/1). *In:* Yukon Exploration and Geology 2021, K.E. MacFarlane (ed.), Yukon Geological Survey, p. 217–265.

Abstract

Penetratively deformed rocks of the Yukon-Tanana terrane and Semenof block, and unfoliated Jurassic-Cretaceous intrusions are exposed in the southern Big Salmon Range of south-central Yukon. A newly mapped area, centred on the Boswell River, is divided into three structural panels by two regional-scale discontinuities, the Little Bear fault and the Sidney Creek fault.

The panel on the northeastern side of the Little Bear fault includes units dominated by metasedimentary rocks (Slate Mountain succession), mafic volcanic and volcaniclastic rocks (Wiley succession), and a varied metasedimentary/metavolcaniclastic unit (Livingstone Creek succession). Each of these is crosscut by intermediate-mafic intrusions of the Simpson Range suite and is therefore Early Mississippian or older. Fossiliferous limestone is interpreted to unconformably overlie phyllite of the Slate Mountain succession. Other units that crop out in this region are Permian augen schist and Cretaceous plutons, including Late Cretaceous quartz monzonite that hosts the Red Mountain Mo porphyry deposit.

The central part of the area, between the Little Bear and Sidney Creek faults, is dominated by mafic volcanic and plutonic rocks of the Sawtooth succession. These are along strike from, and provisionally correlated with the Moose formation of the Boswell assemblage. The Sawtooth succession is overlain by a carbonate and chert-bearing metasedimentary unit (Rosy succession), which hosts a small foliated metagranodiorite intrusion. A younger, as yet undated, mafic metavolcanic unit (Gunsight succession) is locally preserved above the Rosy succession. The metagranodiorite in the Rosy succession formed *ca.* 336 Ma and underwent metamorphic zircon growth in the Early Jurassic (~195 Ma). This zircon growth is interpreted to have accompanied regional, epidote-amphibolite to amphibolite-facies metamorphism and deformation.

Mississippian rocks of the Simpson Range suite dominate much of the southwestern domain. These intrusions crosscut quartzose schist, graphitic phyllite and metabasaltic rocks of the Flat Creek succession, which also hosts Middle Triassic metagabbro.

* David.Moynihan@yukon.ca

All pre-Jurassic rocks in the area are deformed, while post-tectonic intrusions include members of the Early Jurassic Lokken suite, the mid-Cretaceous Quiet Lake batholith and Iron Creek stock, and the aforementioned Red Mountain suite. Most Early Jurassic intrusions are undeformed, but deformation/hydration of some minor phases suggests they were intruded during the waning stages of deformation.

The Sidney Creek fault is cut by the Early Jurassic Sawtooth stock while the Cretaceous Iron Creek stock intruded across the trace of the Little Bear fault. The Little Bear and Sidney Creek faults are interpreted to define tectonic boundaries between Yukon-Tanana terrane and rocks of the Semenof block and may form part of a regional detachment between these units.

Introduction

This report presents preliminary observations on the geology of the southern Big Salmon Range in south-central Yukon, based on approximately nine weeks of fieldwork conducted over the summers of 2020 and 2021 (Fig. 1; see also Moynihan, 2022). A simplified map and cross sections are presented (Fig. 2), along with brief descriptions and illustrations of the major units, supplemented by some new U-Pb geochronological data. The interpretations included in the report are preliminary and subject to refinement following further analytical work.

The mapped area (approximately 785 km^2) is located east of the Teslin River in the southern Big Salmon Range (Fig. 1; Moynihan, 2022). It encompasses an

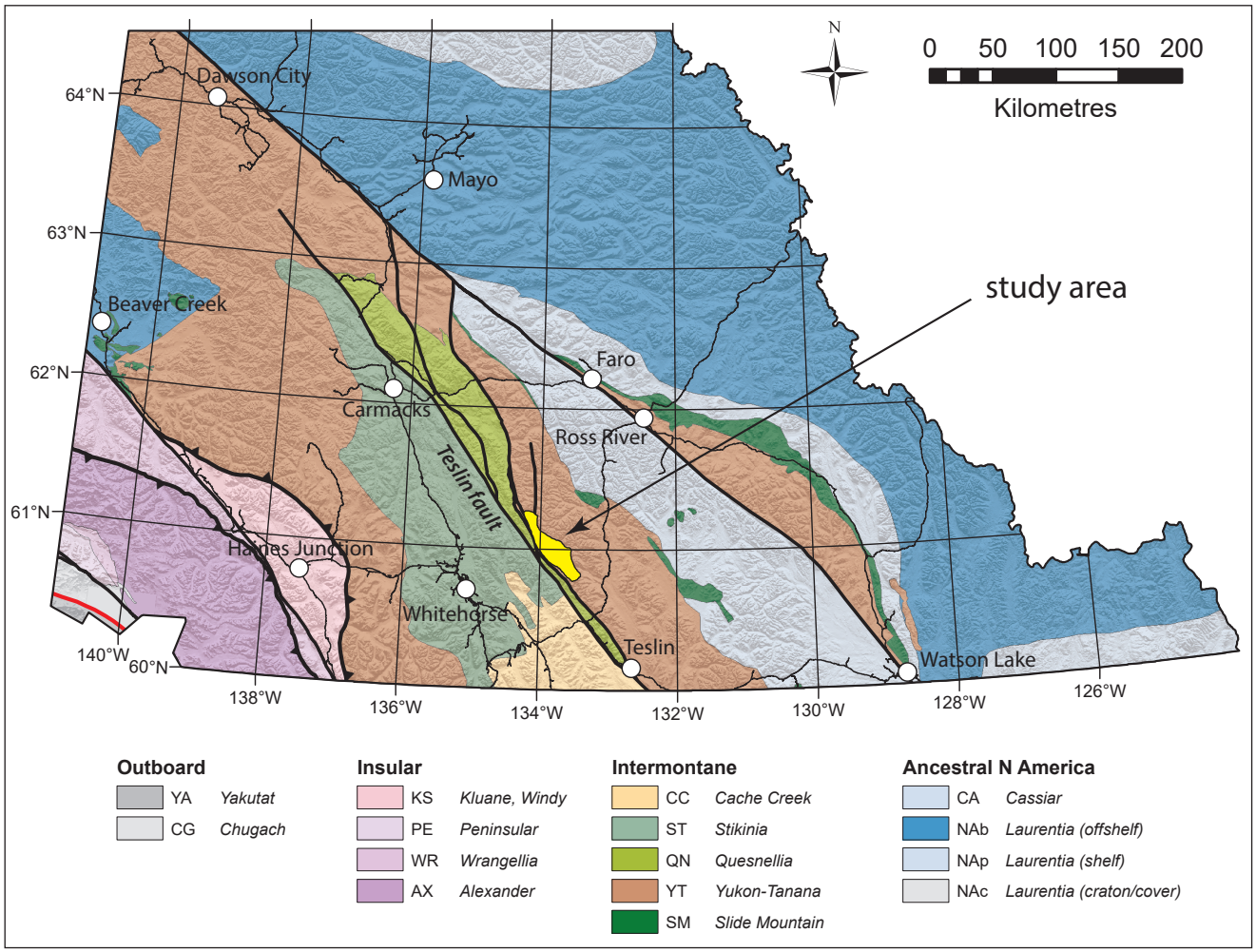

Figure 1. *Terrane map of Southern Yukon (after Colpron and Nelson, 2011). The study area is located approximately 75 km northeast of Whitehorse, east of the Teslin fault. It is mostly underlain by rocks of Yukon-Tanana terrane and the Semenof block.*

elongate NW-SE-trending strip that extends from the South Big Salmon River to upper parts of the Sidney Creek drainage (Fig. 2). The area is centred on the Sawtooth Range and the upper parts of the Boswell River; it includes parts of the Teslin (105C), Quiet Lake (105F) and Laberge (105E) map sheets.

Geological background and previous work

Early accounts of the geology of the area, based on reconnaissance mapping (1:253,440), were provided by Cockfield *et al.* (1936), Lees (1936) and Mulligan (1963); Tempelman-Kluit (1984) subsequently extended 1:250 000-scale mapping in the Lake Laberge and Carmacks areas. The first detailed (1:50 000 scale) mapping of the study area was carried out by Stevens (1994; see also Gordey and Stevens, 1994). The geology of the Semenof Hills was mapped at 1:50 000 by Simard (2003) and is described in Simard and Devine (2003). Colpron (2005a,b, 2006) and Colpron *et al.* (2017) documented the geology of the Livingstone Creek area, directly north of the study area.

The present work builds on Stevens (1994); it aims to provide more detail on the character, age and affinity of lithological units, to provide a clearer understanding of its relationships with other parts of Yukon-Tanana terrane, and to consider implications for metallogenic potential of the southern Big Salmon Range.

The study area is underlain by rocks of the Yukon-Tanana terrane and the Semenof block (Colpron *et al.*, 2003, 2006a). Yukon-Tanana includes: 1) Proterozoic-Devonian metasedimentary rocks that are interpreted to have been rifted from the Laurentian margin, and 2) metavolcanic, metasedimentary and metaplutonic rocks that formed in arc and back-arc environments that developed on and around the rifted basement during the middle to late Paleozoic. The pre-Late Devonian basement is referred to as Snowcap assemblage, while three younger, widely developed unconformity-bounded assemblages have been recognized throughout Yukon-Tanana: 1) the Late Devonian-Early Mississippian Finlayson assemblage, 2) Middle Mississippian-Early Permian Klinkit assemblage and 3) the Middle to Late Permian Klondike assemblage (Colpron *et al.*, 2006a). The Finlayson assemblage is coeval with two voluminous metaplutonic suites – the Late Devonian-Early Mississippian Grass Lakes suite (*ca.* 365–357 Ma) and Early Mississippian Simpson Range suite (*ca.* 355–345 Ma).

The 'Semenof block' (Colpron *et al.*, 2003, 2006a) includes the Semenof hills, which are along strike to the northwest of the study area. Rocks of the Boswell assemblage (Tempelman-Kluit, 1984, 2009; Simard and Devine, 2003) underlie this area. The Boswell assemblage is coeval with parts of Yukon-Tanana but its relationship with it is uncertain (Colpron *et al.* 2006a). Contacts between Yukon-Tanana and the Semenof block are tectonic, and while there are some stratigraphic similarities, particularly between their respective Mississippian-Pennsylvanian successions, definitive correlations have not been established (Colpron *et al.* 2006a).

The oldest part of the Boswell assemblage is Early Mississippian mafic and minor felsic volcanic rocks of the Moose formation. This is overlain by the Boswell formation, which includes sandstone, conglomerate, minor mafic volcanic rocks and one or more prominent Late Mississippian-Early Permian limestone units. The Moose formation is intruded by Late Mississippian-Pennsylvanian hornblende tonalite of the Kelly suite (*ca.* 335–310 Ma), which is similar in age to the Tatlmain suite of Yukon-Tanana (*ca.* 340–336 Ma). Late Triassic rocks of the Semenof Formation, which have been assigned to Stikine (Colpron *et al.*, 2002, 2003) or Quesnel terranes (Gordey and Makepeace, 2001; Colpron *et al.*, 2016) unconformably overlie the Boswell assemblage (Simard, 2003).

The boundary between Yukon-Tanana and the Semenof block is marked by the Big Salmon fault and Needlerock thrust to the north of the study area. Colpron *et al.*, (2003) interpreted the Needlerock thrust to be an early (Triassic-Jurassic) structure that is cut by the Big Salmon fault. The Big Salmon fault truncates the Late Cretaceous Carmacks Group near Little Salmon Lake, which demonstrates some Late Cretaceous or younger movement along at least part of its trace. The Teslin fault marks the western boundary of the Semenof block and Yukon-Tanana terrane at the latitude of the study area (Fig. 1).

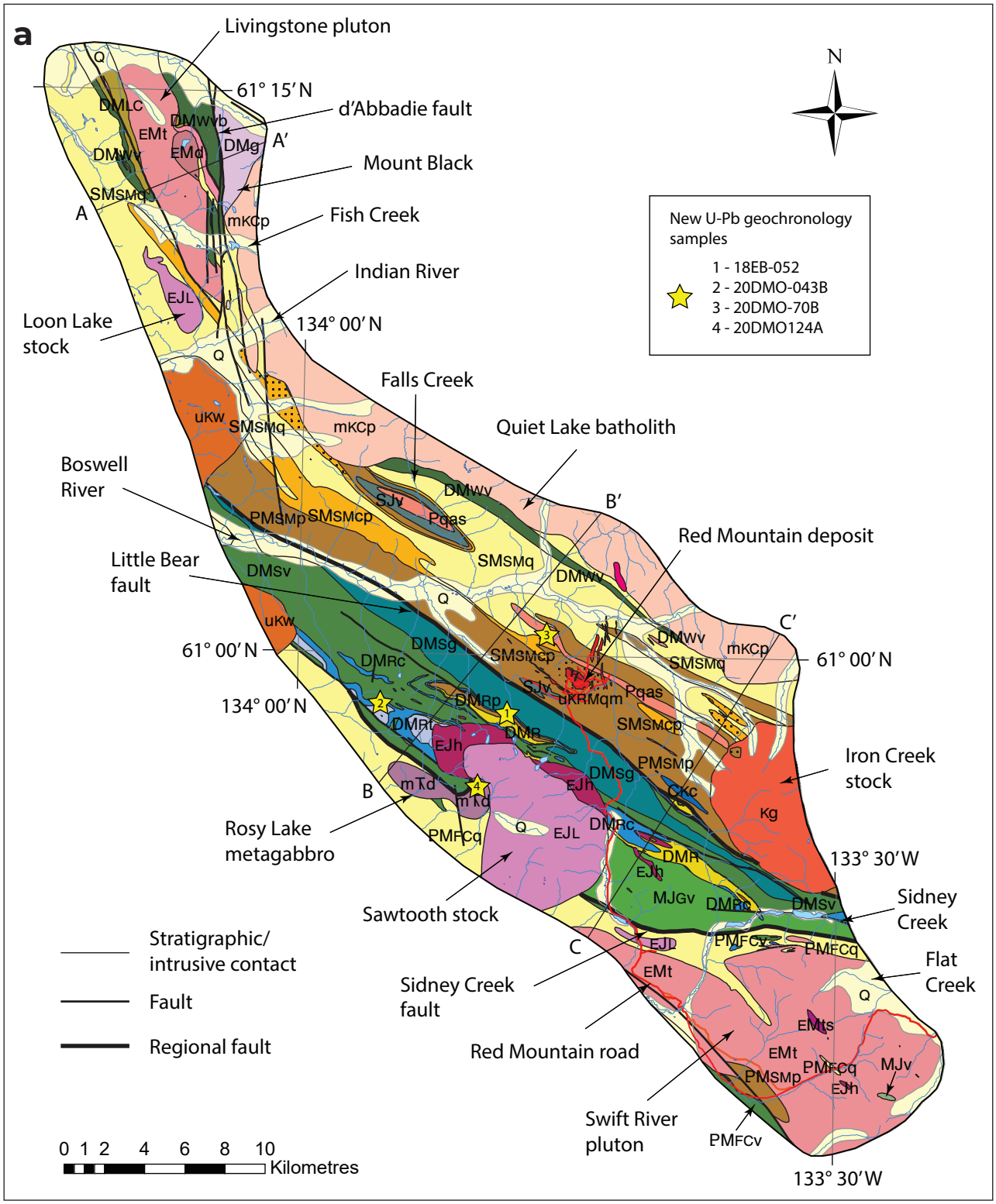

Figure 2. *Simplified geological map* **(a)**, *legend* **(b)** *and cross sections* **(c)** *of the study area (after Moynihan, 2022). Features and places named in the text are shown on the map. Legend and cross sections on following pages.*

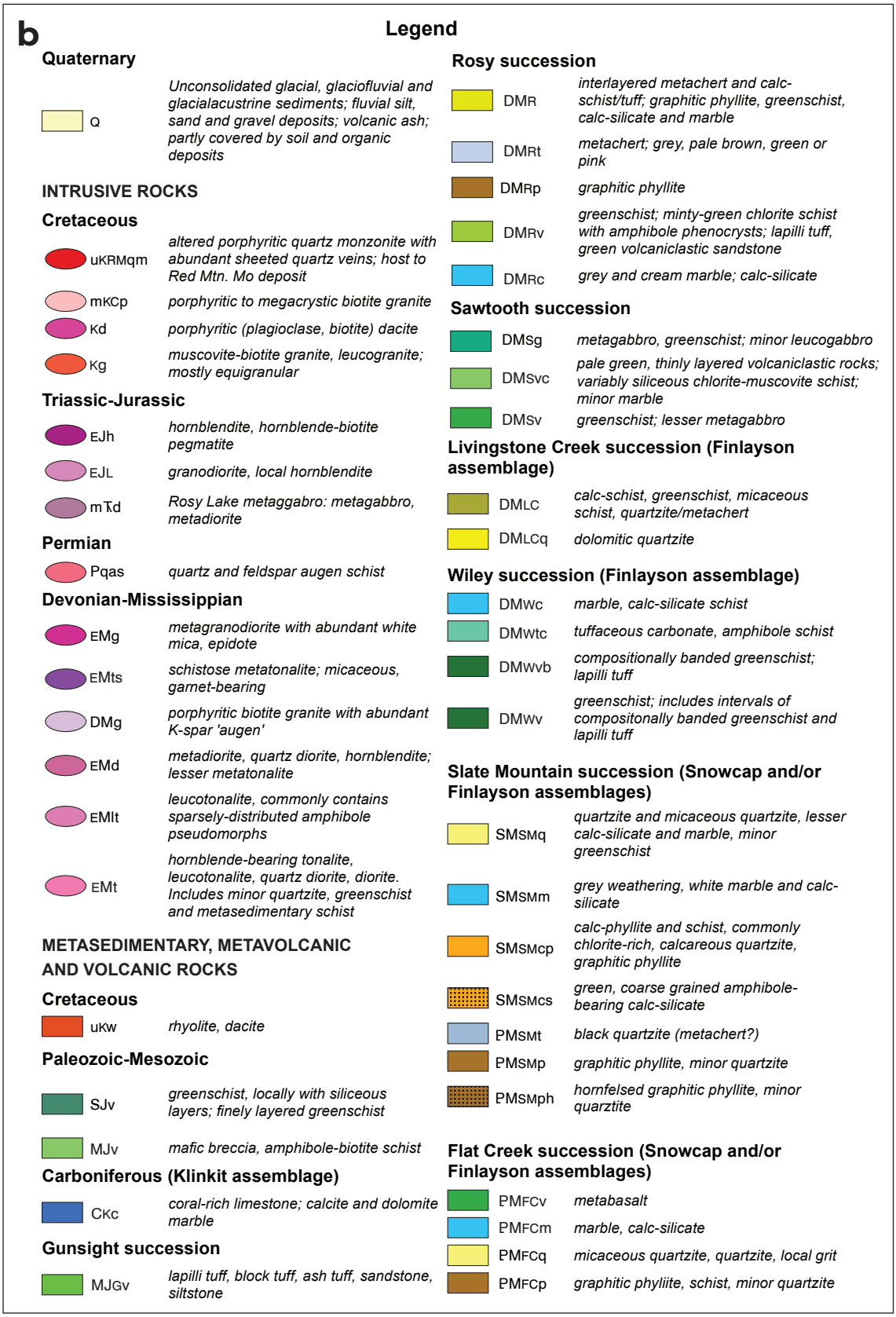

Figure 2 continued. ***(b)*** Legend.

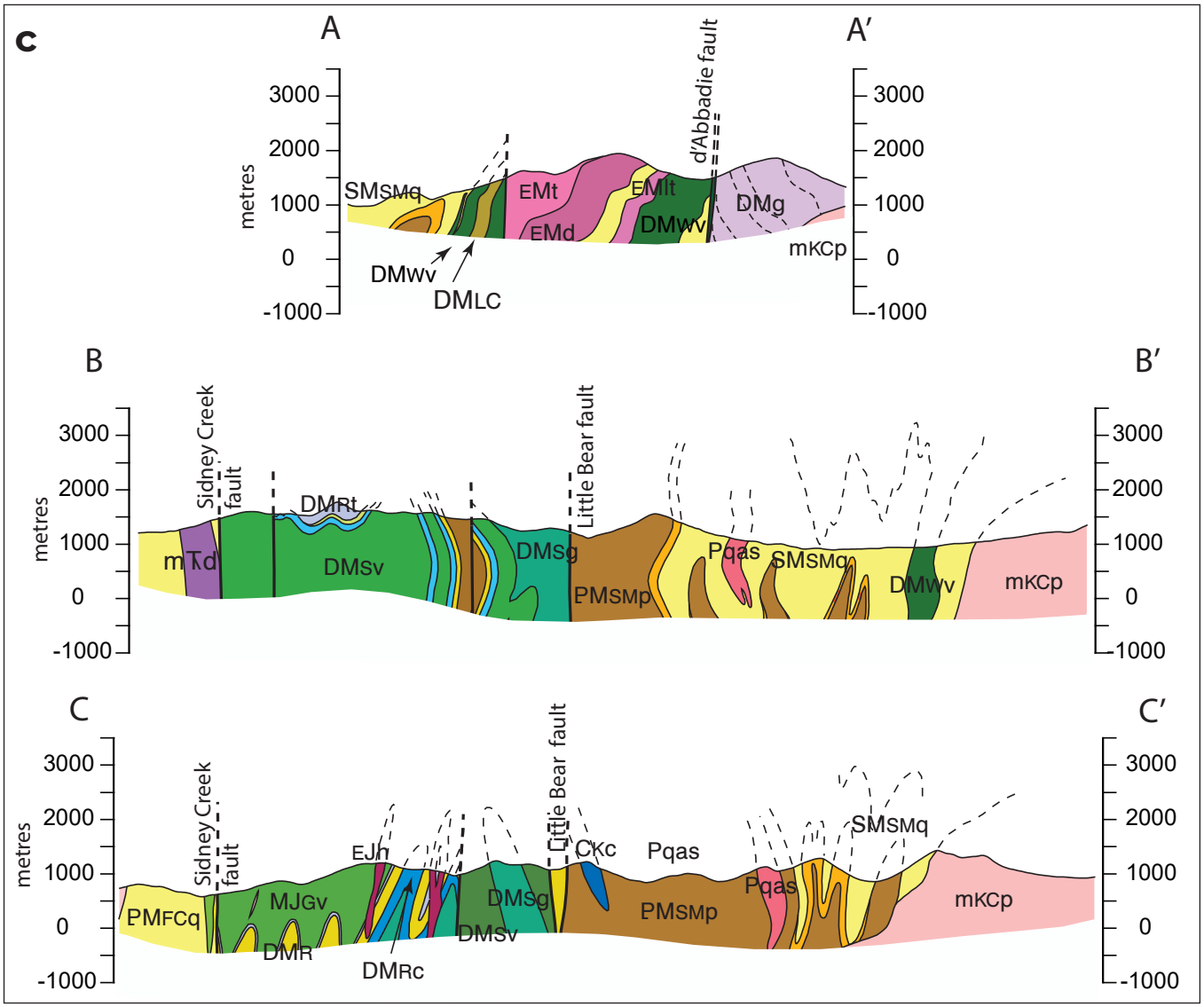

***Figure 2** continued. **(c)** Cross sections.*

Tripartite division of the study area

The mapped area is divided into three belts by the Little Bear and Sidney Creek faults (Figs. 2 and 3). The Little Bear fault separates Mississippian metaplutonic and older metasedimentary/metavolcanic rocks in the northeast from a central belt that is dominated by greenschist and metagabbro. The central region also includes some metasedimentary rocks but almost entirely lacks deformed intermediate-felsic intrusions. The Sidney Creek fault marks the southwestern boundary of the central belt and juxtaposes this region against an area dominated by intermediate Mississippian metaplutonic and older metasedimentary rocks. All three belts host largely undeformed Cretaceous intrusions (Fig. 3). The central belt is interpreted to form part of the Semenof block, while the outer regions are parts of Yukon-Tanana terrane.

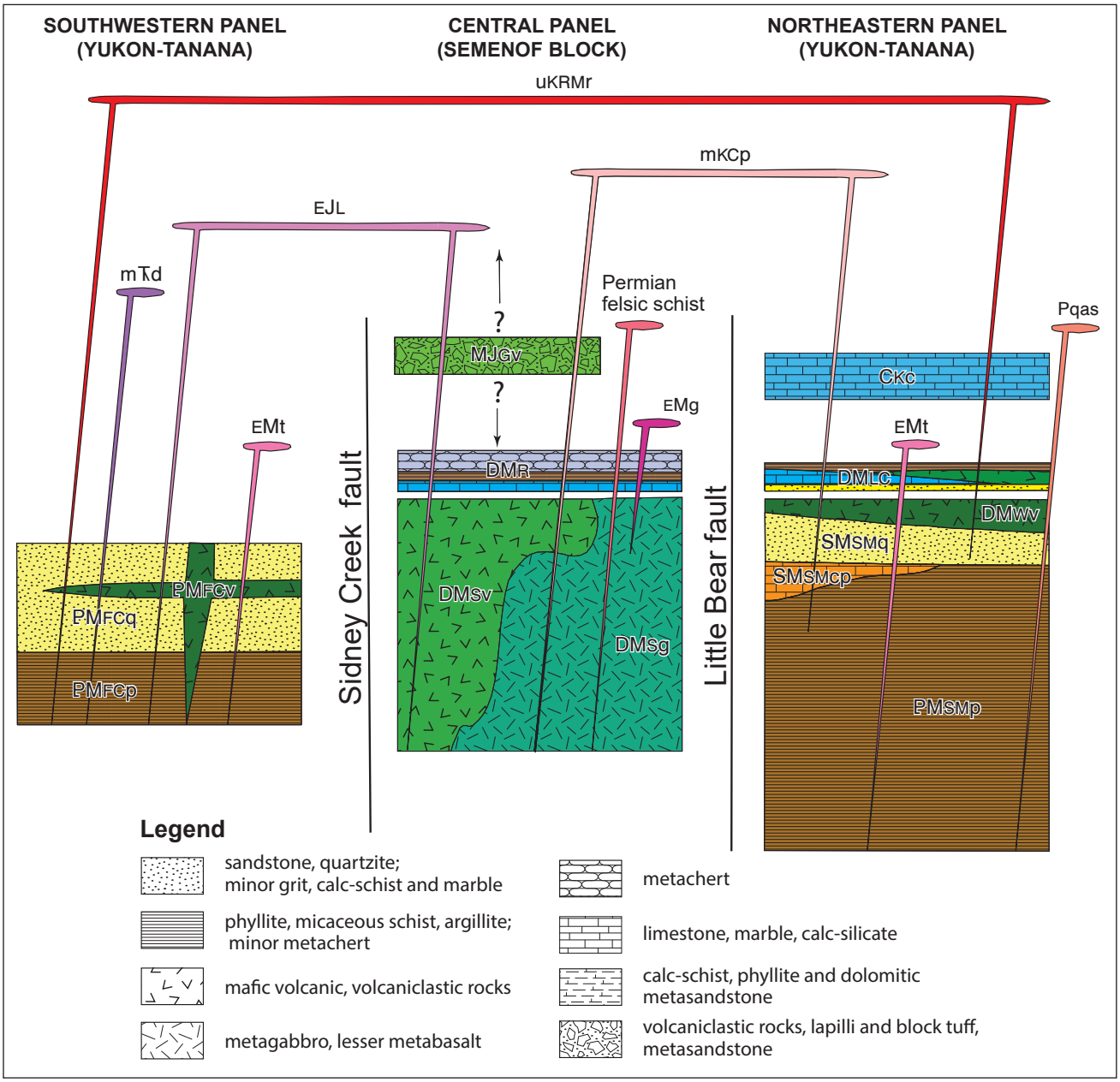

Figure 3. *Provisional interpretation of relationships between major stratigraphic and intrusive units, with relative time on the Y-axis. The Little Bear and Sidney Creek faults divide the area into three structural domains. The southwestern and northeastern domains are dominated by metasedimentary successions that are intruded by plutons assigned to the Simpson Range suite, while the central region is dominated by mafic metavolcanic/plutonic rocks and lacks Simpson range suite intrusions. Jurassic intrusions are interpreted to crosscut the Sidney Creek fault.*

Metasedimentary and metavolcanic rocks northeast of the Little Bear fault (Yukon-Tanana terrane)

Slate Mountain succession

The Slate Mountain succession is a belt of folded metasedimentary rocks that crops out between the Little Bear fault and the Quiet Lake batholith (Fig. 2), and extends the length of the mapped area. It includes three main map units: 1) a dark phyllite unit, 2) a calc-schist/calc-silicate unit, and 3) a unit dominated by metasandstone. There are gradational lithological changes between these units in many parts of the area.

Dark phyllite (PMSMp)

Much of the region immediately northeast of the Little Bear fault is underlain by dark, carbonaceous phyllite and argillite (Fig. 4a). The phyllite is typically medium grey, dark grey or black and weathers rusty brown. A particularly dark, graphite-rich interval is exposed near the top of Slate Mountain, southeast of the Boswell River. This unit also includes numerous thin (5–15 cm thick) layers of quartzite that contain dark graphitic folia, and locally metre-scale intervals of homogeneous, finely banded grey to black quartzite that may represent metamorphosed chert (Fig. 4b). Sooty grey limestone/marble is also a minor constituent.

Chloritic calc-schist/calc-silicate (SMSMcp)

The dark, graphitic phyllite is in gradational contact with a widely, but discontinuously distributed unit that includes a mix of calcareous and siliciclastic rocks in varying ratios. The most distinctive rock type is a finely layered calc-schist that comprises folia of green, chlorite-rich phyllite/schist interlayered with tan to orange weathering dolomitic siliceous layers (Fig. 4c,d). This rock type commonly hosts abundant carbonate and quartz-carbonate veins. Other varieties include similar calc-schist in which the phyllitic layers are mostly grey rather than green, and intervals that are dominated by grey phyllite with sparse green and tan calcareous/dolomitic layers. Locally, the unit includes relatively pure grey weathering, white to buff marble within calc-schist/silicate intervals. Similar rocks were reported by Colpron (2006) and Westberg (2010) in the Dycer Creek succession north of Mendocino Creek (NTS 105E/8 and 105F/5).

Near the Quiet Lake batholith, this unit was metamorphosed to higher grade and is represented by green, splintery calc-silicate/skarn. The rock is medium to coarse grained, pale to medium green and is compositionally banded (Fig. 4e,f). It is dominated by quartz, plagioclase and green amphibole and/or pyroxene; it also contains K-feldspar and locally pale pink garnet.

Quartzite/micaceous quartzite (SMSMq)

This unit is dominated by micaceous quartzite, with lesser, relatively pure quartzite. Micaceous quartzite weathers beige to pale brown and is mostly grey on fresh surfaces (Fig. 4g). It contains abundant closely spaced, wispy and discontinuous to continuous micaceous folia, and is sometimes characterized by subtle cm-scale colour banding (mostly tones of grey, cream, beige and pale brown). Relatively pure quartzite forms resistant ribs that weather white (Fig. 4h). Micaceous folia are thin and widely spaced (~1 cm); fresh surfaces are pale grey and glassy. Other rock types in this unit include minor pale grey calc-silicate and rare decimetre to metre-scale marble and calc-silicate bands. Pebble conglomerate was also observed in a single locality. Outcrops on slopes above the Boswell River, near the contact with phyllite/calc-schist unit, include intervals of tan weathering metasandstone with thin grey or green (chlorite-rich) folia. This suggests a gradational boundary between the quartzite (SMSMq) and calc-schist (SMSMcp) units. Farther northeast, the quartzite includes thin bands of biotite-bearing greenschist. It is unclear whether this represents part of a stratigraphic transition into the Wiley succession, or is the result of tight infolding. The contact with the Wiley succession is otherwise discrete and is commonly marked by a discontinuous band of white marble and impure calc-silicate marble. The marble is grey weathering, white on fresh surfaces, and commonly 5 to 10 m thick.

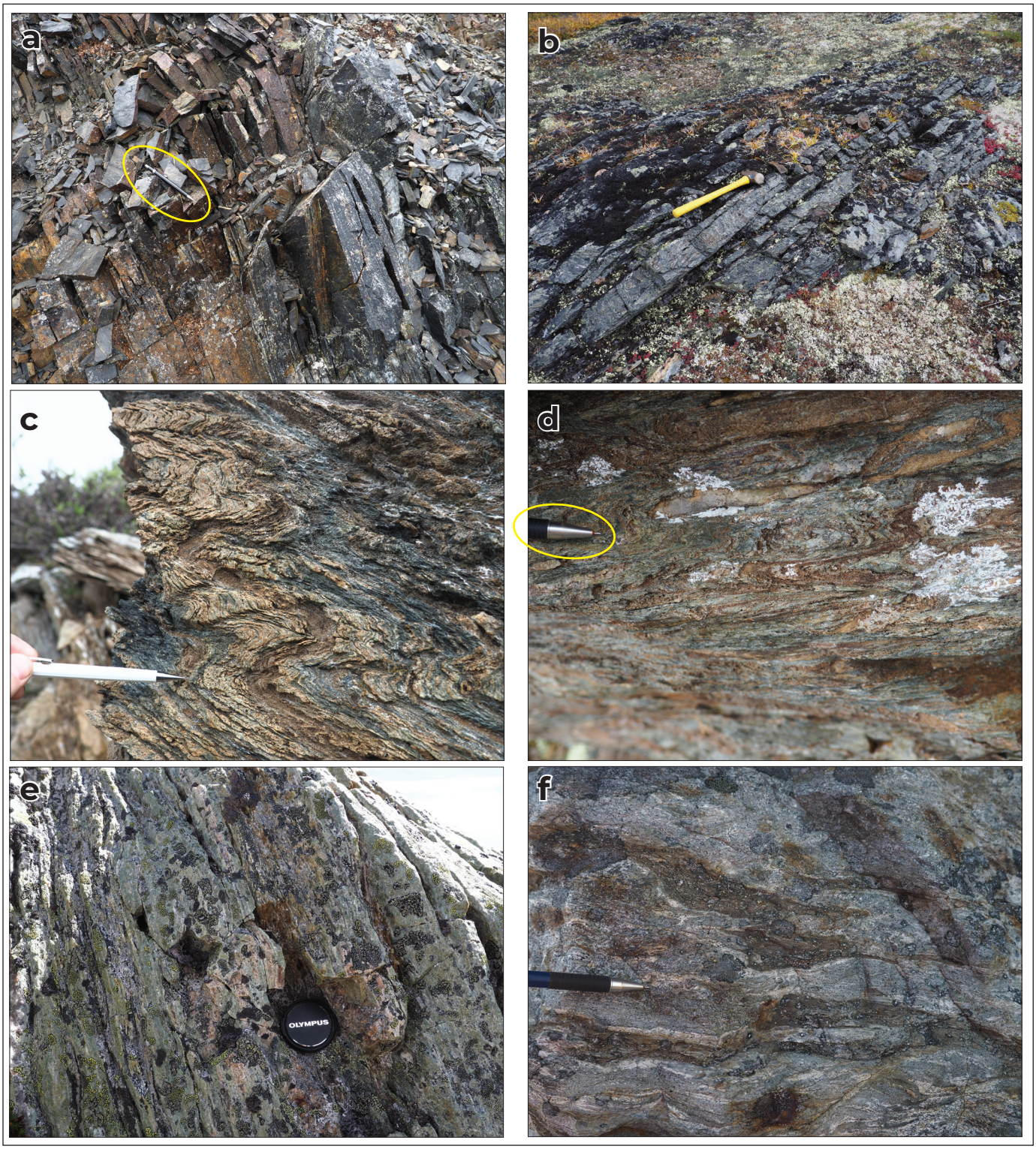

Figure 4. *Slate Mountain succession field photographs.* ***(a)*** *Dark grey, rusty weathering argillite; pencil for scale.* ***(b)*** *Thinly layered dark grey to black, thinly banded quartzite, possibly metachert; hammer for scale.* ***(c and d)*** *Chloritic calc-schist, composed of alternating layers of tan coloured, dolomitic cemented metasandstone, and green or grey, chlorite-rich phyllite; pencil for scale.* ***(e)*** *Banded green calc-silicate with pale pink garnet near the boundary of the Quiet Lake batholith; lens cap for scale.* ***(f)*** *Folded calc-silicate with irregular compositional domains; pencil for scale.* *Figure continued on next page.*

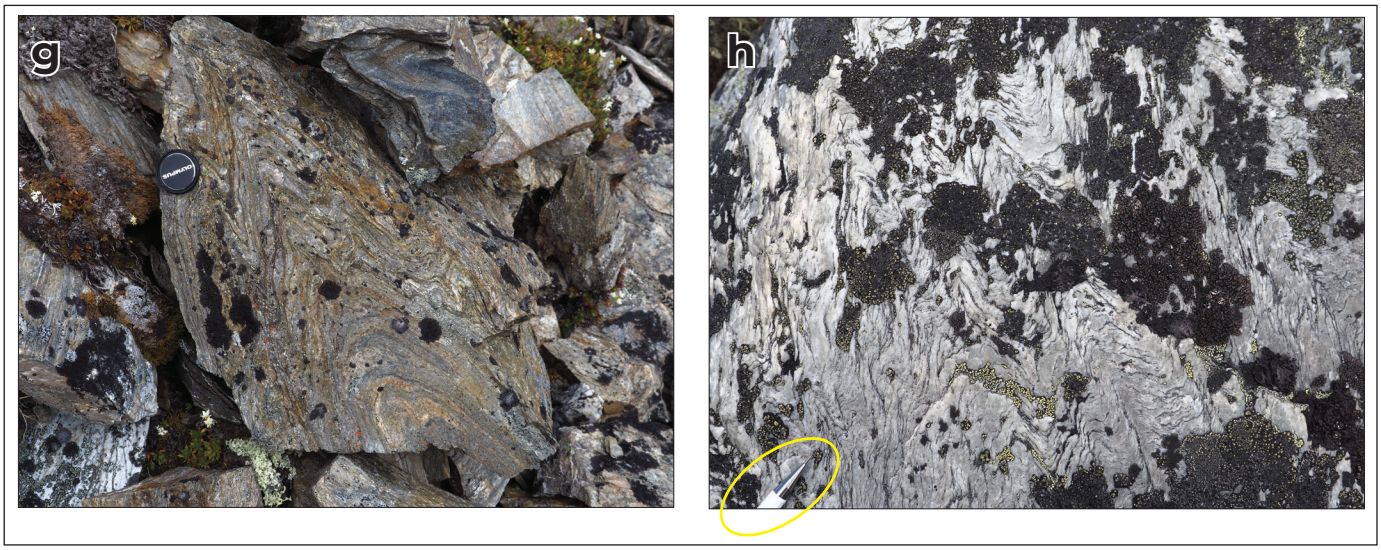

***Figure 4** continued.* ***(g)** Folded micaceous quartzite; lens cap for scale.* ***(h)** White weathering quartzite with widely spaced micaceous folia; pencil tip in lower left corner for scale.*

Age constraints and correlation

The Slate Mountain succession is along strike from, and apparently continuous with similar units in the Livingstone Creek area. The dark phyllite, calc-schist and quartzite units are correlated with PDSp, PDSv and PDSq (Colpron, 2017), respectively. SMSMq is physically continuous with, and therefore correlative with the "Loon Lake" succession of Barresi (2004).

There are few direct constraints on the age of the Slate Mountain succession. The quartzite is intruded by tonalite-granodiorite of the Early Mississippian Simpson Range suite, and small dikes of similar composition were observed in each of the other two units. There is no evidence concerning the relative age of the units, but based on regional patterns, it is likely that PMSMp is the oldest unit, and SMSMq, which is in direct contact with greenschist of the Wiley succession, is younger.

The black phyllite and calc-schist units are interpreted to form part of the Snowcap assemblage, while the quartzite could form part of the Snowcap or Finlayson assemblages. A possible along-strike correlative to the southeast is the Swift River Group of northern British Columbia/southernmost Yukon (Gleeson *et al.*, 2000; Roots *et al.*, 2006).

Wiley succession (DMWv)

There is extensive exposure of greenschist in the northern part of the map area, around the margins of the Livingstone pluton (Fig. 2). Another band of greenschist runs close to the margin of the Quite Lake batholith, in the Boswell River drainage. Each of these belts of greenschist is in contact with rocks of the Slate Mountain succession (quartzite unit) and are assigned to the Wiley succession. The greenschist is mostly medium to dark green (weathered) and dark green fresh. It is commonly banded, with millimetric alternations of dark green layers (rich in chlorite and amphibole) and pale layers rich in plagioclase or its replacement products (epidote, clinozoisite; Fig. 5a). The plagioclase rich layers can be relatively continuous or discontinuous lensoidal streaks. This banding is interpreted to result from solid state segregation during metamorphism and deformation. Hematite-stained surfaces are common, and malachite staining is locally developed.

Greenschist on the west side of the d'Abbadie fault (between the fault and the Livingstone pluton) is more varied, and exhibits abundant evidence for reworking of volcanic rocks (Fig. 5b,c). It includes lapilli tuff and finely banded epiclastic metasandstone. It also includes a 2–3 m band of dusty grey, amphibole rich marble near the top of the unit (Fig. 5d).

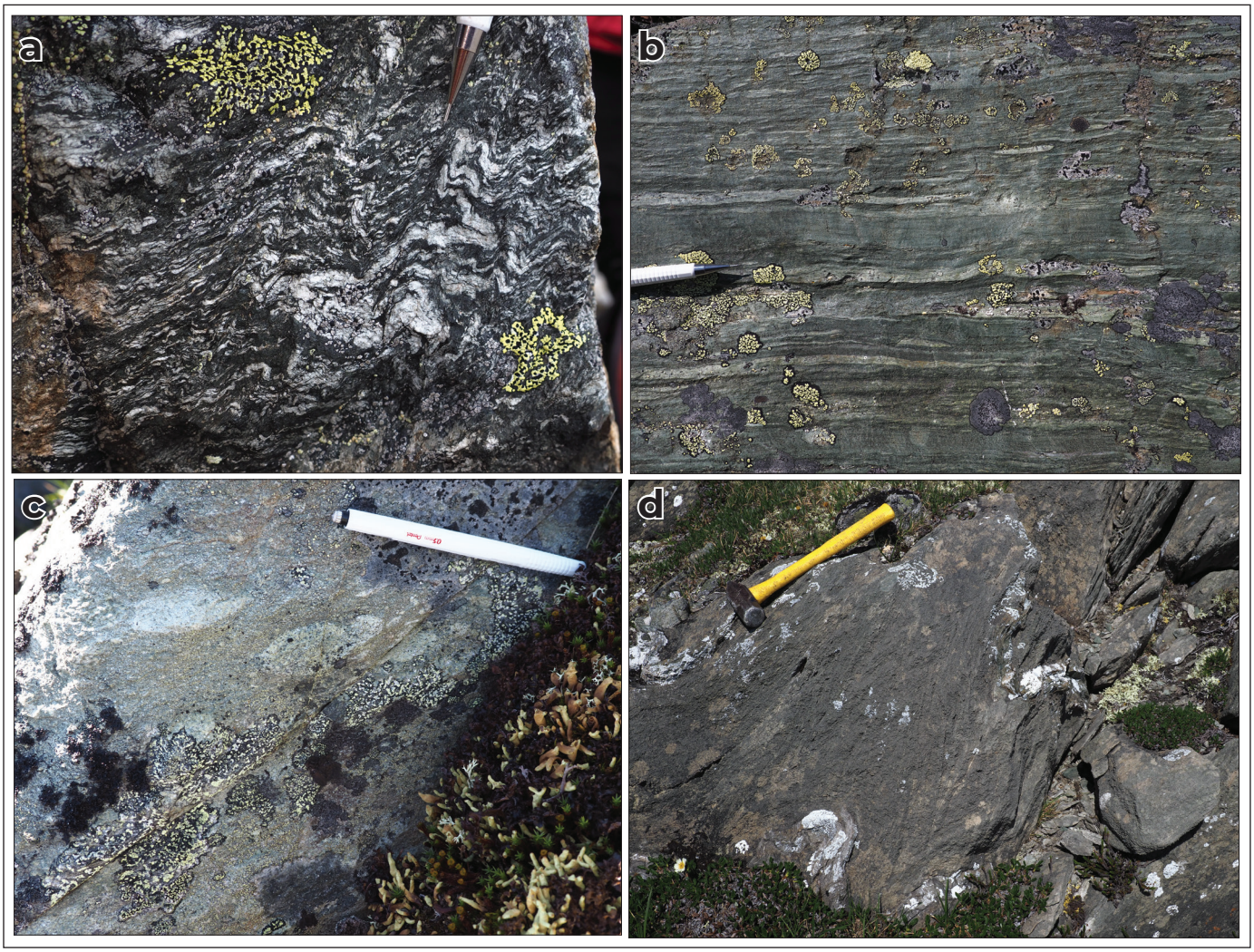

Figure 5. *Wiley succession field photographs.* ***(a)*** *Coarse-grained, segregated amphibolite with refolded folds of plagioclase-rich layers; pencil tip for scale.* ***(b)*** *Layered greenschist with stretched clasts visible in some layers; pencil for scale.* ***(c)*** *Lapilli tuff with centimetre-scale clasts in a matrix of finer grained mafic volcanic detritus; pencil for scale.* ***(d)*** *Folded grey amphibole-rich calc-silicate/marble; hammer for scale.*

Age constraints and correlation

The Wiley succession is interpreted to be intruded by rocks assigned to the Simpson Range suite and is therefore considered to be Early Mississippian or older. It is tentatively interpreted to form part of the Finlayson assemblage of Yukon-Tanana terrane.

Livingstone Creek succession (DMLC)

West of the d'Abbadie fault, greenschist of the Wiley succession is in contact with a distinctive marker unit, approximately 5–10 m thick, which is composed of calcareous (dolomitic) metasandstone and calc-silicate (Fig. 6). The rock weathers white, tan, creamy brown and pale orange and contains abundant coarse carbonate veins. The rock exhibits centimetre-scale layering and has a pitted appearance, caused by the weathering out of recessive carbonate around quartz-rich domains. This passes westward (with contact not exposed) into pale green, amphibole-rich schist.

On the west side of the Livingstone pluton, the Wiley succession is in contact with a mixed package of rocks that includes thin intervals (metres to tens of metres) of

Figure 6. *Basal unit of the Livingstone Creek succession. Layered dolomitic quartzite has a pitted texture caused by preferential weathering out of carbonate in some horizons; pencil for scale.*

many rock types. Lithological units include calc-schist and calcareous quartzite, greenschist, biotite-bearing greenschist with distinctive plagioclase spots, chlorite-muscovite schist, calc-schist and amphibole (chlorite-muscovite) schist.

These rocks are assigned to the Livingstone succession, which was defined by Harvey et *al.* (1997) on the north side of the South Big Salmon River. It is cut by the Livingstone pluton and otherwise only in contact with the Wiley succession. The limited and fragmented nature of its outcrop in the study area inhibits understanding of the distribution of rock types within this unit.

The Livingstone Creek succession is Early Mississippian or older, and was correlated with the Little Kalzas formation of the Finlayson assemblage (Colpron et *al.*, 2006b) by Colpron (2006).

Falls Creek and Red Mountain greenschist (SJv)

There are two regions of greenschist on the east side of the Little Bear fault that have an anomalous relationship to surrounding units; rather than being in contact with quartzite or separated from it by a thin marble, they are in direct contact with graphitic phyllite. The first of these is west of Falls Creek (Fig. 2).

Sulphide-rich greenschist includes intervals of finely banded rock, with mm to cm-scale, sharp to gradational alternations between chlorite-rich schist and siliceous layers. This is interpreted as depositional layering and rules out an intrusive origin for the rock. The Falls Creek greenschist is interpreted to be either 1) unconformable on the Slate Mountain succession, or 2) a local volcanic facies in the approximate stratigraphic position of the calc-schist unit. This greenschist is in contact with Permian augen schist and is therefore older than *ca.* 262 Ma (see below).

Another variety of greenschist in contact with graphitic phyllite was mapped by Taylor (1975) southwest of the Red Mountain deposit, close to the trace of the Little Bear fault; these rocks were described as chlorite schist, chlorite + graphite schist, talc-chlorite schist and talc-sericite schist. Only one outcrop in this area was visited, where graphitic phyllite is intercalated with pale green chloritic phyllite. Faint, thinly layered banding in the chloritic phyllite suggests a volcaniclastic origin for the rock, but further study is needed to better characterize the unit.

Fossiliferous limestone (CKcP)

A thick limestone/marble unit is preserved in a synformal keel directly northeast of the Little Bear fault, near the northwestern boundary of the Iron Creek stock. It overlies graphitic phyllite, and there is some interlayering of phyllite and calc-silicate near the base of the unit. A distinctive layer in the transition zone includes lenses/pods of yellow and orange carbonate in a phyllitic matrix. Most of the carbonate is relatively pure, fully recrystallized cream coloured calcite or dolomite marble, but patches of dark grey limestone are preserved (Fig. 7a). These darker grey regions contain chert bands and are highly fossiliferous, with abundant boundstone (Fig. 7b). Fossils include colonial corals, but formal analysis and identification has not yet been carried out.

The fossiliferous limestone is interpreted to be unconformable on the dark phyllite unit, and may be correlative with the Carboniferous, fossiliferous English Creek/Screw Creek limestone of the Klinkit assemblage (Simard et *al.* 2003; Roots et *al.*, 2006), which is widely distributed along strike to the southeast.

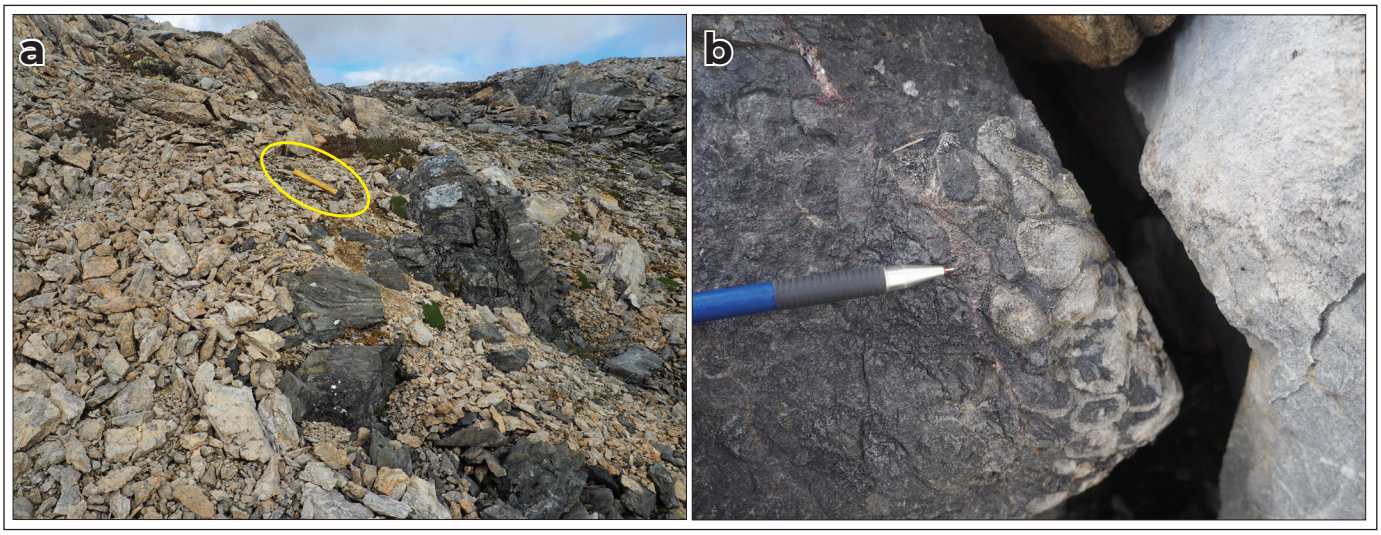

Figure 7. *Fossiliferous limestone field photographs.* ***(a)*** *Enclave of dark grey fossiliferous limestone surrounded by talus and outcrop of fully recrystallized, dolomitic marble.* ***(b)*** *Cross sectional view through coral boundstone; pencil for scale.*

Metasedimentary, metavolcanic and mafic metaplutonic rocks between the Little Bear and Sidney Creek faults (Semenof block)

Sawtooth succession (DMSv, DMSg)

The northeastern flanks of the Sawtooth Range are underlain by greenschist (metabasalt) and metagabbro. The greenschist is medium to dark green and weathers rusty brown. It is chlorite rich (Fig. 8a), phyllitic to schistose, and in some locations exhibits compositional banding, with pale layers/lenses composed of plagioclase and/or its replacement products (e.g., clinozoisite) that alternate with dark green, chlorite, epidote and amphibole-rich domains (Fig. 8b). It locally includes porphyritic tuffaceous layers (Fig. 8c). The greenschist has high to very high magnetic susceptibility (locally up to 80 SI units). Hematite-stained surfaces are common in the greenschist, and malachite staining was locally observed. Greenschist is foliated throughout, but is particularly strongly foliated and banded near boundaries with marble of the overlying Rosy succession. Locally, at or near the top of the greenschist (near its contact with the Rosy succession), there is a white to orange brown weathering, more plagioclase-rich, strongly banded unit that is interpreted as a metamorphosed and deformed interval of volcaniclastic rock (Fig. 8d). This interval also includes some siliceous chlorite-muscovite schist and thin impure marble layers.

Metagabbro is typically medium to very coarse (Fig. 8e), texturally highly variable (Fig. 8f), and commonly weathers white. Local varieties include metagabbroic pegmatite (Fig. 8g) and leucogabbro. It is mostly foliated but variably deformed, with relatively weakly deformed pods surrounded by anastomosing arrays of more highly foliated domains. Typically, metagabbro retains its igneous texture, with plagioclase and pyroxene crystals pseudomorphed by clinozoisite and amphibole-rich domains, respectively. Locally, Cr-rich mica is also developed. In regions of high strain, including some contacts with the Rosy succession, there is a progressive reduction in grain size and metagabbro is transformed to a pale green, chlorite-rich schist.

The boundaries between greenschist and gabbro-dominated regions are commonly gradational, and each contains a minor proportion of the other lithology; gabbroic domains locally include abundant thin screens of metabasalt (Fig. 8h), while there are numerous small gabbro plugs within greenschist-dominated regions. Nevertheless, they form separate map units, and their folded contact defines structures, e.g., the upright antiform north of Sidney Creek.

Figure 8. *Sawtooth succession field photographs.* ***(a)*** *Crenulated chlorite-rich greenschist; pencil for scale.* ***(b)*** *Banded greenschist with tightly folded, plagioclase-rich and poor layers; pencil tip for scale.* ***(c)*** *Plagioclase phenocrysts in a tuffaceous horizon within the Sawtooth succession greenschist unit.* ***(d)*** *Fine-grained, strongly banded interval, interpreted as a volcaniclastic horizon near the top of the Sawtooth succession; pencil for scale.* ***(e)*** *Coarse-grained, foliated metagabbro. Igneous minerals have been replaced but the primary texture is preserved; pencil for scale.* ***(f)*** *Medium to coarse-grained foliated metagabbro with varying grain size and degrees of strain; hammer for scale.* *Figure continued on next page.*

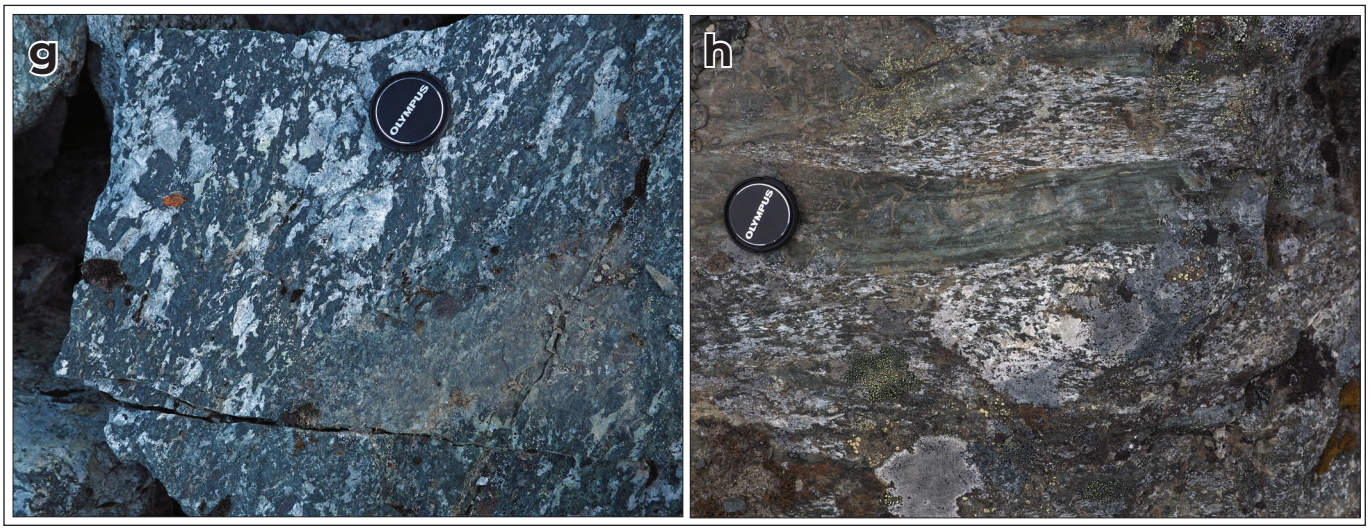

***Figure 8** continued.**(g)** Greenschist enclave in metagabbro, with apparent truncation of the compositional layering; lens cap for scale. **(h)** Metagabbroic pegmatite with cm-scale crystals; lens cap for scale.*

Ultramafic rocks form a negligible proportion of the Sawtooth succession; metre-scale serpentinite pods after metagabbro were observed near the Iron Creek pluton/Little Bear fault, and a few metres of carbonate-altered (?) ultramafic rock is developed along a fault that cuts the greenschist unit south of the Boswell River.

Correlation of the Sawtooth assemblage with the Moose formation

Metavolcanic rocks on the southwestern side of the Little Bear fault have relatively high magnetic susceptibility, whereas metasedimentary rocks on its northeastern side are mostly non-magnetic (Fig. 9). This gives rise to a prominent linear aeromagnetic boundary, which is a geophysical proxy for the fault trace. The fault and its associated aeromagnetic feature extend northwestward from the mapped area into a region, approximately 6 km wide, which is underlain by Late Cretaceous volcanic rocks (80 ± 2.3 Ma; Stevens *et al.*, 1982).

A similar arrangement is evident on the northwestern side of the Late Cretaceous volcanic belt. Here, mafic volcanic rocks of the Moose and Semenof formations are juxtaposed, across the trace of the Big Salmon fault (*sensu* Stevens, 1994; Simard *et al.* 2003; Colpron, 2006a), with non-magnetic metasedimentary rocks of the Loon Lake succession, resulting in a similar aeromagnetic contrast.

The fault and lithological boundaries on either side are collinear, and are interpreted to be continuous under the unconformably overlying Late Cretaceous volcanic rocks. This interpretation is supported by linear aeromagnetic features that pass into and out of the Cretaceous volcanic rocks without deflection. The Slate Mountain succession can be traced continuously on the eastern side of the Little Bear fault into rocks, on the eastern side of the Big Salmon fault, that were assigned to the Loon Lake succession by Barresi (2004). Based on these relationships, the Moose formation and Sawtooth succession are provisionally interpreted to be adjacent parts of the same metavolcanic unit.

There are no direct constraints on the age of the Sawtooth succession, but three U-Pb dates constrain the age of the Moose formation. A quartz-feldspar porphyritic rhyolite at the top of the formation yielded a date of approximately 359 ± 3 Ma (based on 2 concordant fractions out of 5; Yukon Geological Survey (YGS), 2021). Another sample from the same rhyolite member produced a date of 352.1 ± 1 Ma, with one of three fractions concordant. Southwest of Loon Lakes, the Moose formation is intruded by hornblende diorite and by pink and green, locally quartz-porphyritic granite. The granitic phase, which is the later of the two phases yielded a date of 347.0 ± 1.2 Ma, with three of six fractions concordant. Farther north, near Little Salmon Lake, a fine-grained quartz diorite that was interpreted to be comagmatic with basalt, yielded a slightly younger date of 342.8 ± 2.2 Ma (YGS, 2021).

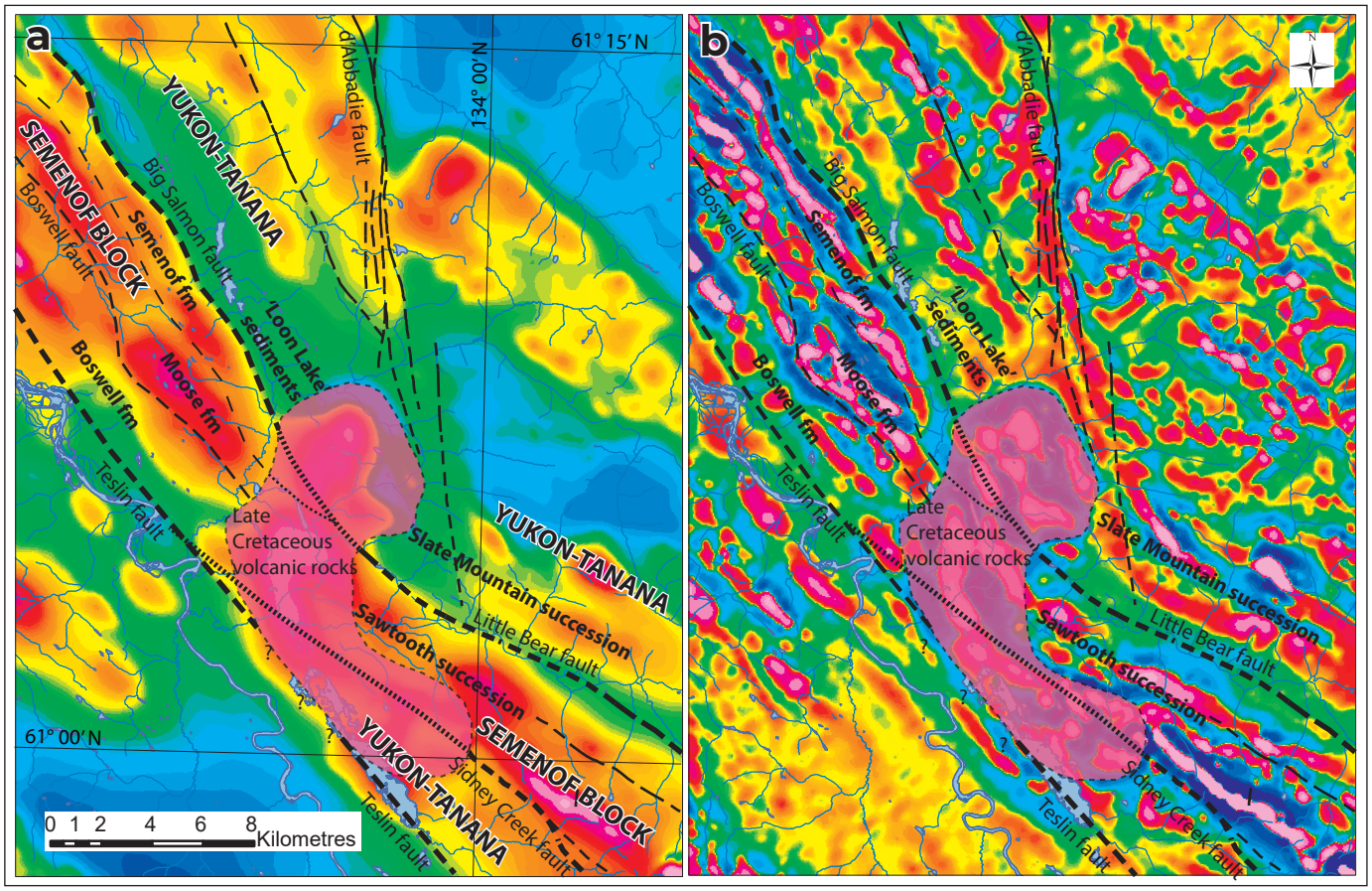

Figure 9. *Residual* ***(a)*** *and second derivative* ***(b)*** *results from the Marsh Lake aeromagnetic survey (Kiss and Boulanger, 2018), covering the northwestern part of the study area and the southern Semenof Hills. Interpreted faults and contacts are shown. The Sawtooth succession is interpreted to be correlative with the Early Mississippian Moose formation, which lies along strike to the northwest. The southern tip zone of the d'Abbadie fault is in the region N-NE of the Late Cretaceous rocks. The southwestern boundary of the Late Cretaceous volcanic belt may coincide with the Teslin fault. Geology of the area NW of the Cretaceous volcanic rocks is from Simard (2003) and Colpron (2017).*

Rosy succession (DMRc, DMRt, DMR)

Gabbro and greenschist of the Sawtooth succession are each in contact with a pale marble/calc-silicate unit that forms the base of the Rosy succession. Marble is mostly white or cream and pale grey weathering (Fig. 10a). Impure parts of the unit are white, cream or tan, with abundant brown weathering micaceous folia between marble bands, or pods of white, columnar tremolite/wollastonite.

In some places, a relatively pure marble/calc-silicate is up to 20 m thick, but elsewhere, the basal Rosy succession consists of thin (metre-scale) alternations of pale marble, quartz-rich white or green calc-silicate (Fig. 10b), and calc-schist. In part of the Sawtooth Range an orange-brown dolomitic breccia forms a thin band surrounded by greenschist. This likely represents an isoclinal infold of the basal Rosy succession, rather than a unit that is stratigraphically within the Sawtooth succession.

Although a basal marble/calc-silicate unit is ubiquitous, the overlying Rosy succession is variable. On the east flank of the Sawtooth Range, basal marble and calc-silicate pass upward through a thin interval (10–15 m) of greenschist and striped siliceous rock (metachert?) into tens of metres of dark graphitic phyllite. Locally, the phyllite contains thin sooty limestone/marble layers (Fig. 10c).

On the western flank of the Sawtooth Range (NW of the Sawtooth stock), marble becomes impure upsection, with abundant thin grey siliceous layers alternating with white to tan marble/calc-silicate (Fig. 10d). The mixed siliceous/carbonate is overlain by thinly layered siliceous rock that is interpreted as metachert (Fig. 10e). The chert ranges from white to brown, is thinly layered, forms platy outcrops, and mostly composed of silica, with some very fine mica crystals on foliation planes. Some thin intervals of greenschist were locally observed near the base of this unit, but rocks above the metachert are not exposed.

Southeast of the Sawtooth stock, the lower parts of the Rosy succession includes massive marble, but contains a greater proportion of mixed marble with siliceous layers. Marble-dominated rock passes into a characteristic stripy unit that contains cm-scale, alternating bands of siliceous rock (metachert?) and recessive weathering, calcareous bands (Fig. 10f). Graphitic phyllite is also locally exposed in this region.

Calcareous layers in the banded unit are mostly grey, but locally buff coloured. The calcareous bands die out into an interval of thinly layered metachert (Fig. 10g). In close proximity to a hornblendite intrusion, (tuffaceous?) calcareous layers within the banded interval are transformed into recessive-weathering, green amphibole schist (Fig. 10f), and siliceous layers are green or pink (Fig. 10h). The pink colouration is

Figure 10. *Rosy succession field photographs.* ***(a)*** *Pure white, grey weathering marble; pencil-sized eraser for scale.* ***(b)*** *Pale green quartzite and calc-silicate near the base of the Rosy succession; hammer for scale.* ***(c)*** *Dusty grey limestone forms thin layers in graphitic phyllite of the Rosy succession northwest of the Sawtooth stock; pencil for scale.* ***(d)*** *Grey marble with numerous thin (1-5 cm thick) siliceous layers. Pencil for scale.* *Figure continued on next page.*

caused by the presence of pink/fuchsia epidote, which may reflect a high Mn content. In this area, the thin-banded chert, which is mostly white, grey (Fig. 10g) or pale green elsewhere, is pink/mauve (not illustrated).

The lower, calcareous part of the Rosy succession is intruded by Mississippian metagranodiorite (ca. 336 Ma; see below). Contact of the basal carbonate unit with both metagabbro and metabasalt of the Sawtooth succession is suggestive of a primary unconformable relationship, but the nature of the relationship is obscured by high strain.

Gunsight succession (MJGv)

Mafic volcanic and volcaniclastic rocks underlie the region immediately northeast of the Sidney Creek fault, from the southeastern margin of the Sawtooth pluton to the edge of the mapped area. The contact with the Rosy succession is tightly constrained on the ridge immediately northeast of the Red Mountain road but is not exposed. Grey metachert of the Rosy succession is in close proximity to an interval of fine to medium grained volcaniclastic metasediments. Grey-green metasiltstone and metasandstone display internal laminations and cm-scale, locally graded layering. This interval also includes some coarser-

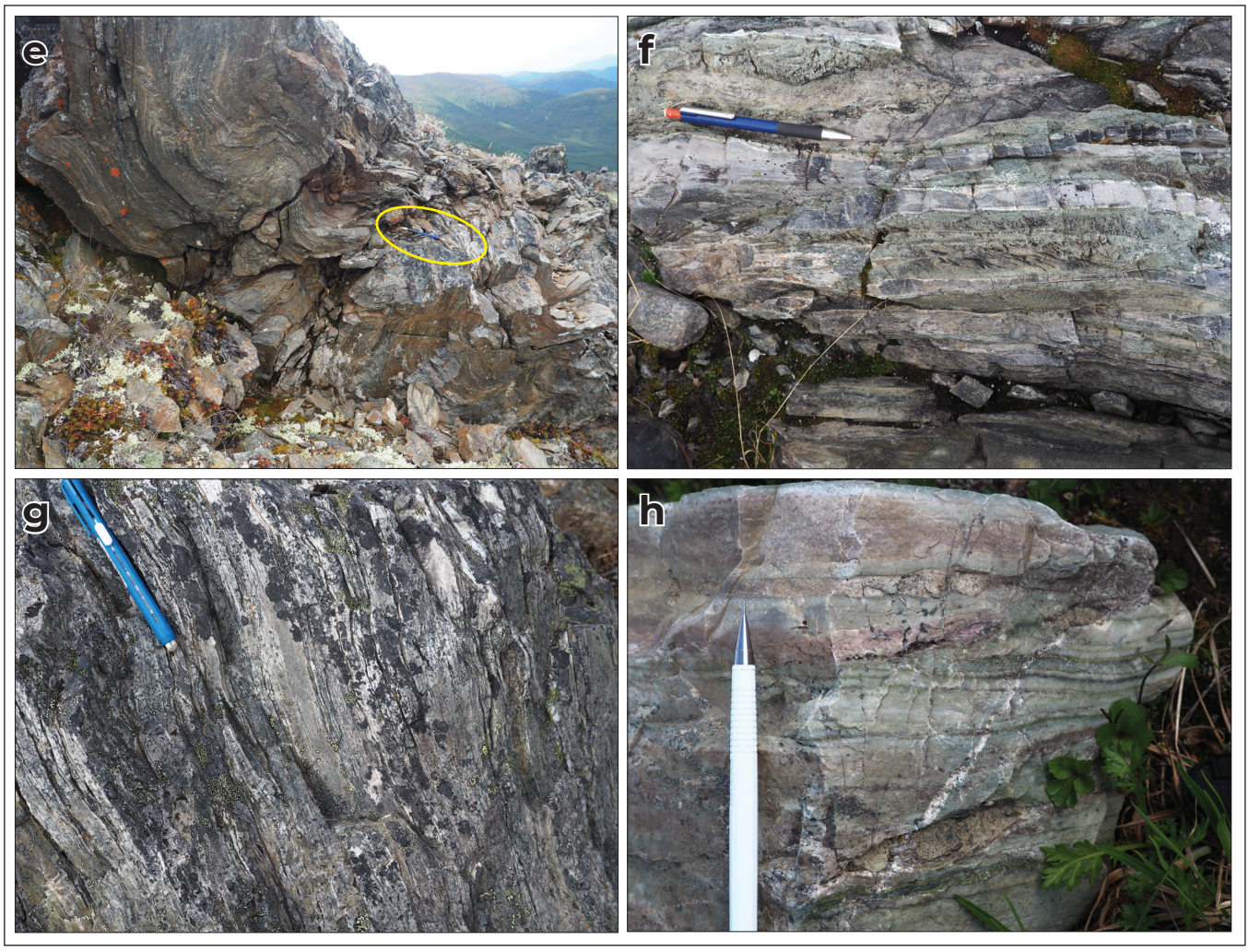

***Figure 10** continued.* ***(e)** Folded brown quartzite, interpreted as metachert, from the northwestern side of the Sawtooth stock; pencil for scale.* ***(f)** Centimetre-scale alternation between grey siliceous layers and green, slightly calcareous (tuffaceous?) amphibole schist; pencil for scale.* ***(g)** Thinly layered interval of white and grey weathering siliceous rock, interpreted as metachert; pencil-sized eraser for scale.* ***(h)** Green chert with some thin calcareous (recessive) layers; pencil for scale.*

grained layers of amphibole-plagioclase schist. This relatively fine-grained interval passes westward into coarser mafic volcaniclastic rocks. Lapilli tuff at the base of the coarse interval includes cm-scale clasts of grey marble in addition to mafic volcanic clasts and sparsely distributed grey chert (Fig. 11a). Recessive weathering of carbonate gives rise to a pitted texture in some layers within this rock. The overlying green-grey to dark grey tuffaceous layers contain lapilli to block clasts, and include discontinuous, wispy layers of ash tuff (Fig. 11b), along with intraclasts of grey to green volcanic metasiltstone/sandstone. The outline of stubby black pseudomorphed (?)pyroxene and plagioclase phenocrysts are preserved, and angular clast outlines are discernable in some of the coarser grained, less foliated horizons (Fig. 11c).

Near the margins (within hundreds of metres) of the hornblendite that intrudes the Gunsight succession, many rocks are massive, black weathering, and grey on fresh surfaces. Elsewhere, the most common rock types include mint green chlorite schist with relic black phenocrysts, green plagioclase-rich metasandstone, and mint green, well foliated lapilli tuff (Fig. 11d).

The Gunsight succession is interpreted to stratigraphically overlie the Rosy succession; It is therefore Mississippian or younger, and could be as young as early Jurassic – the interpreted age of the crosscutting hornblendite body (see below).

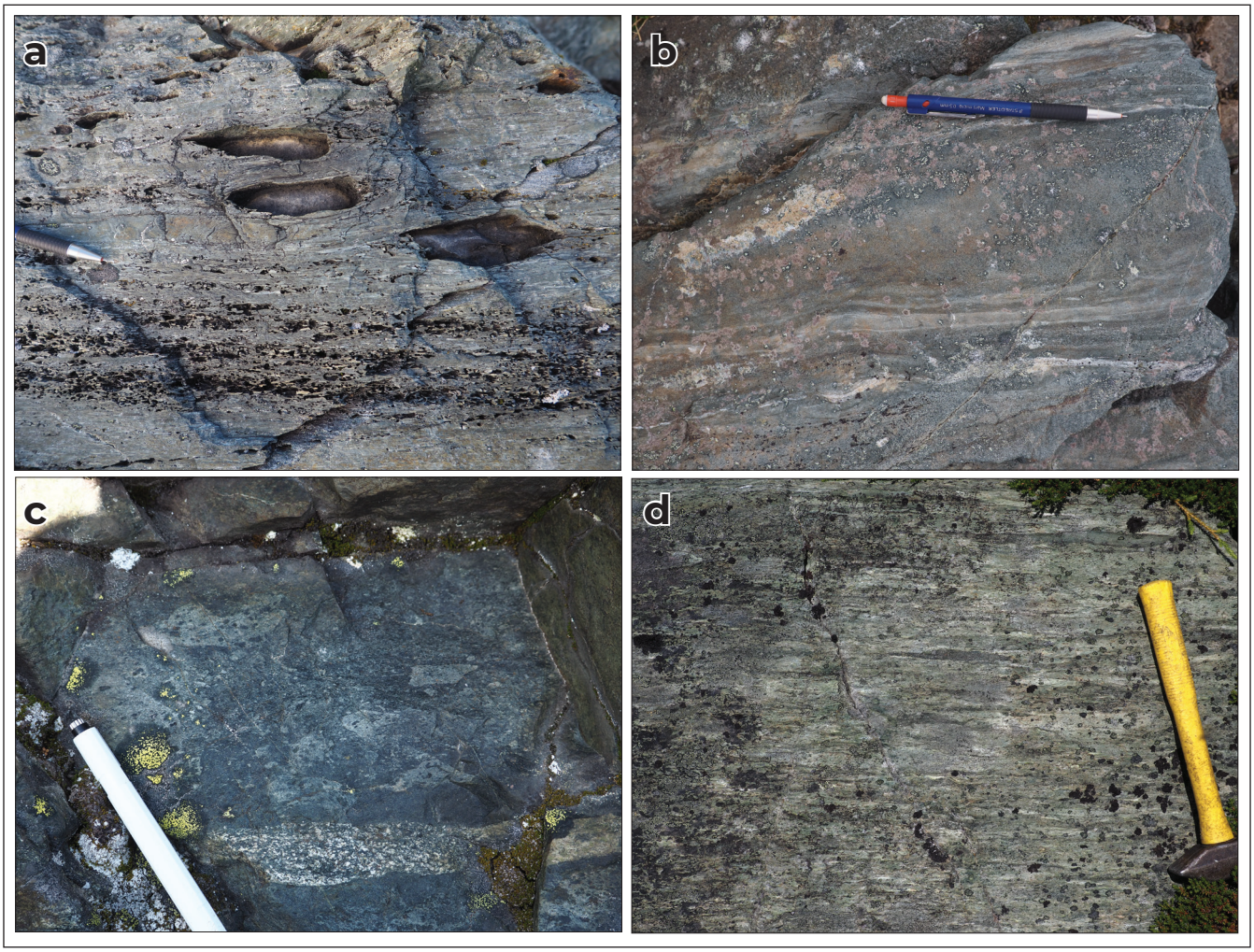

Figure 11. *Gunsight succession field photographs.* ***(a)*** *Lapilli tuff with recessive grey carbonate clasts; pencil for scale.* ***(b)*** *Wispy ash mafic layers near the base of the Gunsight succession; pencil for scale.* ***(c)*** *Angular clasts of clinopyroxene(?) porphyry in a lapilli tuff. The tuff is cut by an undeformed plagioclase-hornblende porphyritic dike, which is interpreted to form part of the Jurassic Lokken suite; pencil for scale.* ***(d)*** *Stretched clasts in green, chloritic lapilli tuff; hammer for scale.*

Metasedimentary and metavolcanic rocks southwest of the Sidney Creek fault (Yukon-Tanana terrane)

Flat Creek succession (PMFCq, PMFCg, PMFCp, PMFCv)

The southern part of the mapped area is dominated by exposures of metaplutonic rocks of the Simpson Range suite (Swift River pluton; Fig. 2). Metasedimentary rocks are exposed around the fringes of the pluton and as a screen within. The most extensive belt of metasedimentary rocks is between the northern margin of the pluton and the Sidney Creek fault. This region is dominated by micaceous quartzite (Fig. 12a), with lesser marble and calc-silicate. The micaceous quartzite is pale shades of beige, grey, green, tan and white, and is grey and glassy on fresh broken surfaces. It contains abundant micaceous foliation surfaces and is locally garnet-bearing. Talus generated from this unit is blocky, has smooth surfaces, and is commonly associated with yellow-orange staining. Foliated 'grit' that is exposed southeast of the Sawtooth stock is also included in the Flat Creek succession (Fig. 12b). The grit comprises thick, homogeneous layers, is cream to tan coloured, poorly sorted, and contains abundant quartz granules.

Marble and calc-silicate (Fig. 12c) form layers and pods that are mostly metres thick, but locally up to 20 m. Marble is white and pale grey weathering, with sparse silicate folia. It is also commonly mixed with white or cream calc-silicate/calc-schist and calcareous quartzite.

The region between the Sidney Creek fault and the batholith also includes two significant regions of amphibolite and garnet amphibolite (Fig. 12d), interpreted as metabasite, with strike lengths >1 km. The (garnet) amphibolite is black, and commonly contains thin (mm to cm-scale) lenses and layers of felsic intrusive rock with sparsely distributed amphibole. The amphibolite is in contact with micaceous quartzite, but the primary relationship (intrusive *vs.* stratigraphic) is unknown.

Metabasite is also exposed on the southwestern flanks of the batholith, near the margin of the mapped area. Here, green, rusty weathering metabasalt forms resistant slabby outcrops with abundant hematite staining. It is in contact with quartz-rich steely grey schist that grades into graphitic phyllite (locally garnet-bearing schist). Outcrops of graphitic phyllite include thin intervals of calc-schist and greenschist.

Varied rocks on the poorly exposed slopes west of the Sawtooth pluton, which host a Triassic metagabbro (described below) include quartz-rich paragneiss with abundant quartzo-feldspathic segregations, garnet amphibolite and deformed felsic-intermediate intrusions. There is also banded (metavolcaniclastic?) rock composed of cm-scale alternations between grey siliceous layers and pale green and grey amphibole/biotite schist, which is intruded by metamorphosed hornblende tonalite/diorite. This amphibole-biotite schist was not observed elsewhere in the Flat Creek succession.

Micaceous quartzite south of the Sidney Creek fault, and graphitic phyllite and greenschist in the southwestern part of the map area are cut by small intrusions of amphibole-bearing metatonalite, possibly of the Simpson Range suite; they are therefore likely to be Early Mississippian or older. The relationship between the graphitic phyllite and the micaceous quartzite/marble unit is not known, nor is the nature of the contacts with greenschist/amphibolite/garnet amphibolite.

Mafic volcanic/volcaniclastic rocks (MJv)

A small region of foliated mafic volcaniclastic rock is in contact with metatonalite of the Simpson Range suite near the southeastern boundary of the map area. This includes mafic lapilli tuff with rare clasts of fibrous serpentinite and quartz clasts. The unit also includes thinly layered amphibole-biotite-plagioclase schist. The mafic unit was either deposited unconformably on the Simpson Range suite prior to deformation that affects both units, or represents a screen within the Swift River pluton.

Figure 12. *Flat Creek succession field photographs.* ***(a)*** *Grey and green quartzite and micaceous quartzite; hammer for scale.* ***(b)*** *Tan weathering 'grit' with prominent quartz grains and granules; pencil for scale.* ***(c)*** *Grey weathering, white marble with resistant-weathering micaceous folia; hammer for scale.* ***(d)*** *Small garnet crystals in black weathering garnet amphibolite; pencil tip for scale.*

Plutonic and metaplutonic rocks

Grass Lakes suite (DMg)

The summit of Mount Black and the ridge leading north from it are underlain by deformed porphyritic two-mica granitic orthogneiss (Figs. 2 and 13a,b). The rock has a spotted appearance, with phenocrysts/porphyroclasts of creamy-yellow weathering K-feldspar in a brown to grey matrix. This is correlated with the Late Devonian-Early Mississippian Grass Lakes suite, which forms extensive sill-like bodies in parts of Yukon-Tanana (Murphy et *al*., 2006). Exposures of this unit north of the mapped area returned latest Devonian U-Pb dates (Hansen et al., 1989; Westberg, 2010; Colpron et *al*. 2017). The Grass Lake suite is cut by Cretaceous granite of the Quiet Lake batholith. As these units form similar topography and rocks are heavily lichen covered, the contact shown on the map is an approximation.

Simpson Range suite (EMt)

Deformed metatonalite and associated rocks are volumetrically significant in two parts of the map area: 1) north of the Indian River, on the northeastern side of the Little Bear fault (Livingstone pluton), and 2) south of the Sidney Creek fault (Swift River pluton). The dominant rock types in these regions are texturally

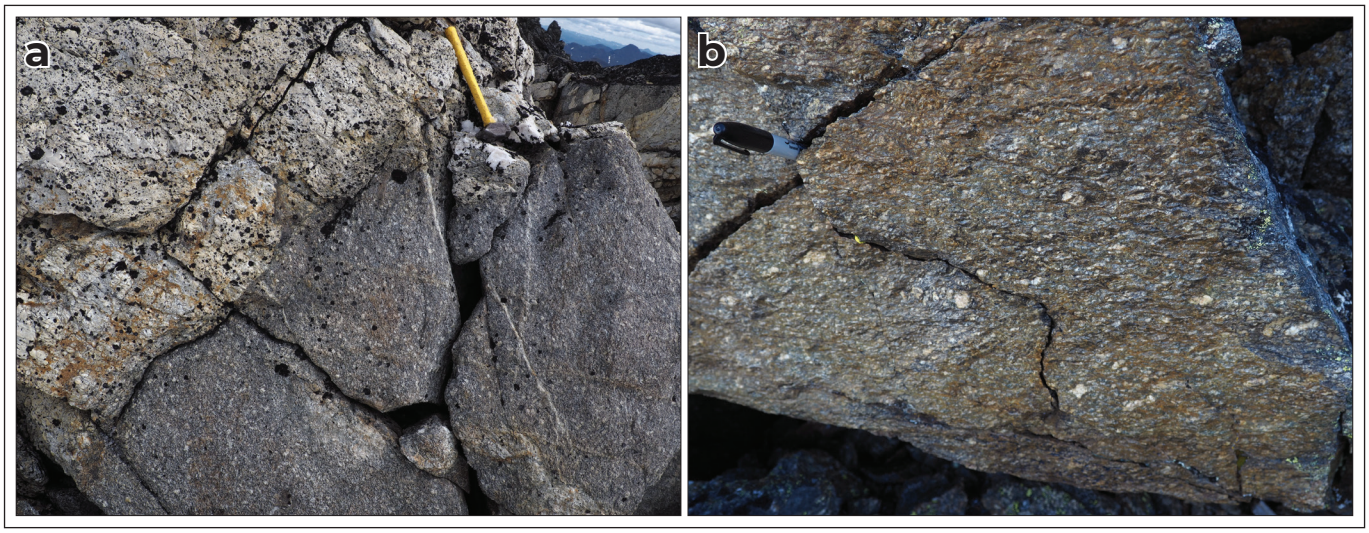

Figure 13. *Grass Lakes suite field photographs.* ***(a)*** *Porphyritic granitic orthogneiss of the Grass Lakes suite cut by undeformed pale yellow Cretaceous granite; hammer for scale.* ***(b)*** *Close-up view of orthogneiss with ~1 cm long K-feldspar crystals wrapped by the foliation; pen for scale visible on extreme left of photograph. Diameter of the pen is ~1 cm.*

and compositionally heterogeneous hornblende metatonalite, metagranodiorite and meta-quartz diorite. Varieties include strained rocks with intact igneous textures, thoroughly recrystallized schists whose protoliths are inferred to be meta-igneous, and intermediate gradations.

Hornblende metatonalite (Fig. 14a) to granodiorite is coarse grained and equigranular or, less commonly porphyritic (Fig. 14b). It is grey-green and weathers white, orange-brown and white, grey or greenish grey. The rock is generally foliated, though non-foliated pods are locally preserved, and is dominated by plagioclase and pseudomorphs of hornblende (now mostly chlorite). Metatonalite is commonly banded or streaky (Fig. 14c,d), characterized by centimetre to decimetre-scale layers or lenses of differing grain size, colour and composition.

Micaceous schists derived from metatonalite-metagranodiorite share the same grey-green colouration and are commonly strongly compositionally banded; they are finer grained, locally weather pale yellow and have a fully recrystallized, metamorphic texture. They have more abundant foliation-parallel quartz veins, and locally include garnet, in addition to plagioclase, quartz, micas and amphibole/chlorite.

The body of metatonalite-granodiorite that underlies the northern part of the area is interpreted to be continuous with the Livingstone pluton, a deformed pluton that underlies a large region in the central part of the Livingstone Creek area to the north (Colpron, 2017). Colpron *et al.* (2017) reported a U-Pb zircon date of 351 ± 1 Ma from metagranodiorite in this pluton. A poorly constrained U-Pb zircon date of 341 +5/-17 Ma was reported by Stevens (1994) for metatonalite of the Swift River pluton. Based on these ages, and characteristics of the rocks, the dominant rock types in these plutons are assigned to the Simpson Range suite. Small intrusions (dikes) of similar rocks were noted in rocks of the Slate Mountain succession and the Flat Creek succession. A single dike of hornblende-bearing diorite crosscuts the Gunsight succession, but it is not known whether this belongs to the Simpson Range, or another, younger plutonic suite.

Part of the eastern flank of the Livingstone pluton comprises banded metadiorite and amphibolite with hornblendite boudins. Outcrops also locally contain abundant deformed pegmatite lenses/layers. This portion of the pluton is broadly coincident with an aeromagnetic high. It is provisionally interpreted as a mafic phase of the Simpson Range suite.

Distinctive leucocratic hornblende metatonalite ('birdfoot leucotonalite') and leucotonalite forms a slender body east of the Livingstone pluton and also forms dikes in its vicinity. Indistinguishable dikes are exposed on the western flanks of the Swift River pluton and leucotonalite forms larger bodies within the Swift River pluton. The characteristic feature of the hornblende leucotonalite (Fig. 14e) is the presence of cm-scale elongate hornblende crystals (now replaced by chlorite) that are sparsely distributed through the rock. Leucotonalite (Fig. 14f) has a medium grained quartzo-feldspathic matrix. It weathers white and is grey-white on fresh surfaces; locally it has a pink/mauve tint and in rare cases contains small (1–2 mm scale) quartz augen. Leucocratic tonalite in the Swift River pluton crosscuts more mafic, hornblende-bearing metatonalite and is therefore, at least locally, a younger phase. In the absence of information to the contrary, the (hornblende) leucotonalite is tentatively interpreted to form part of the Simpson Range suite.

Tatlmain or Kelly suite(?) (EMgd)

A very small (approximately 200 m^2) foliated metagranodiorite intrusion crosscuts the lower, calcareous part of the Rosy succession northwest of the Sawtooth stock. The rock is medium to coarse-grained, weakly porphyritic metagranodiorite with a distinctive pink and green colouration (Fig. 14g).

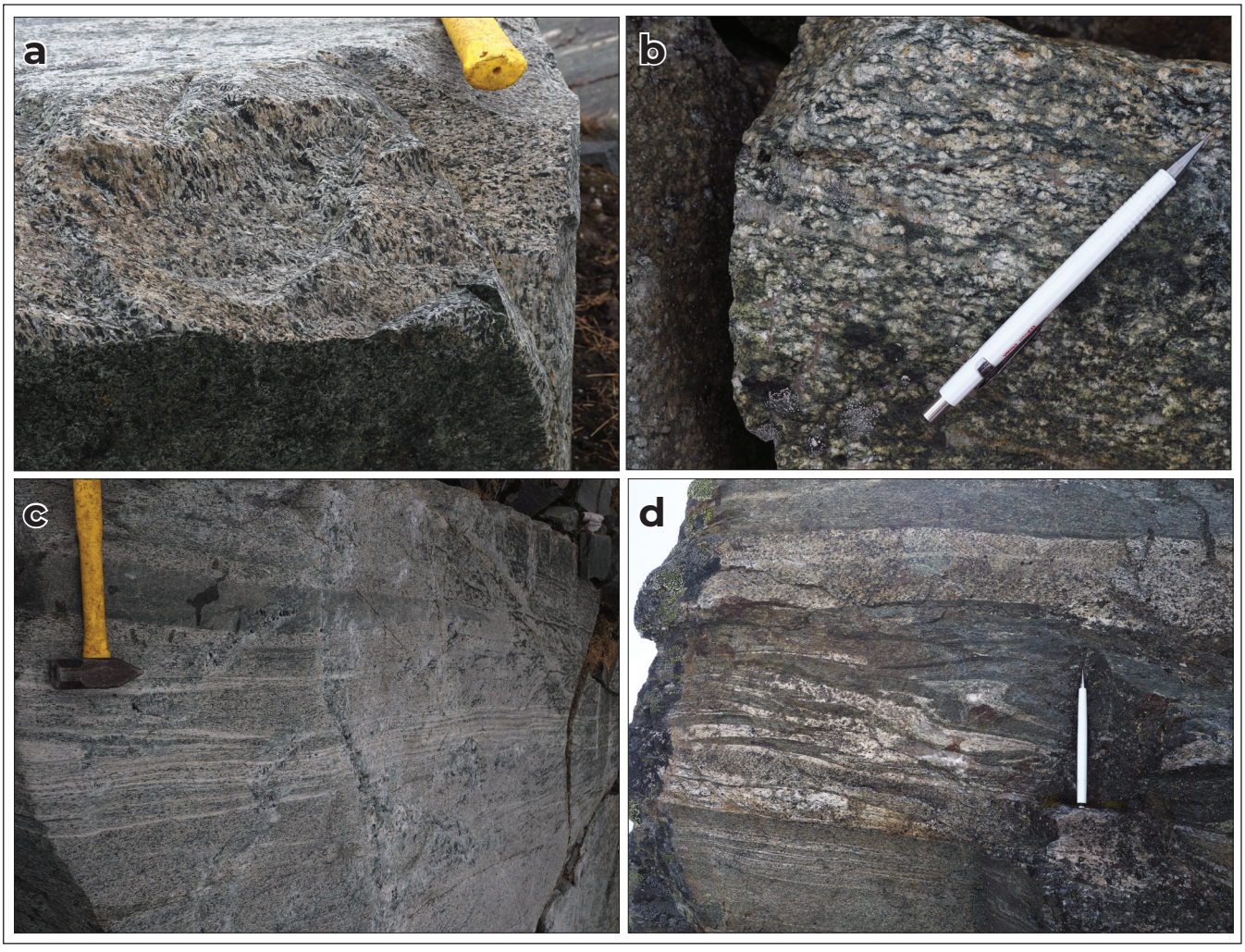

Figure 14. *Simpson Range suite field photographs.* ***(a)*** *Homogeneous, coarse-grained hornblende-bearing metatonalite; hammer for scale.* ***(b)*** *Porphyritic hornblende granodiorite; pencil for scale.* ***(c)*** *Compositionally layered, foliated metatonalite; hammer for scale.* ***(d)*** *Heterogeneous banded metatonalite composed of intrusive sheets of varying composition and grain size; pencil for scale. Figure continued on next page.*

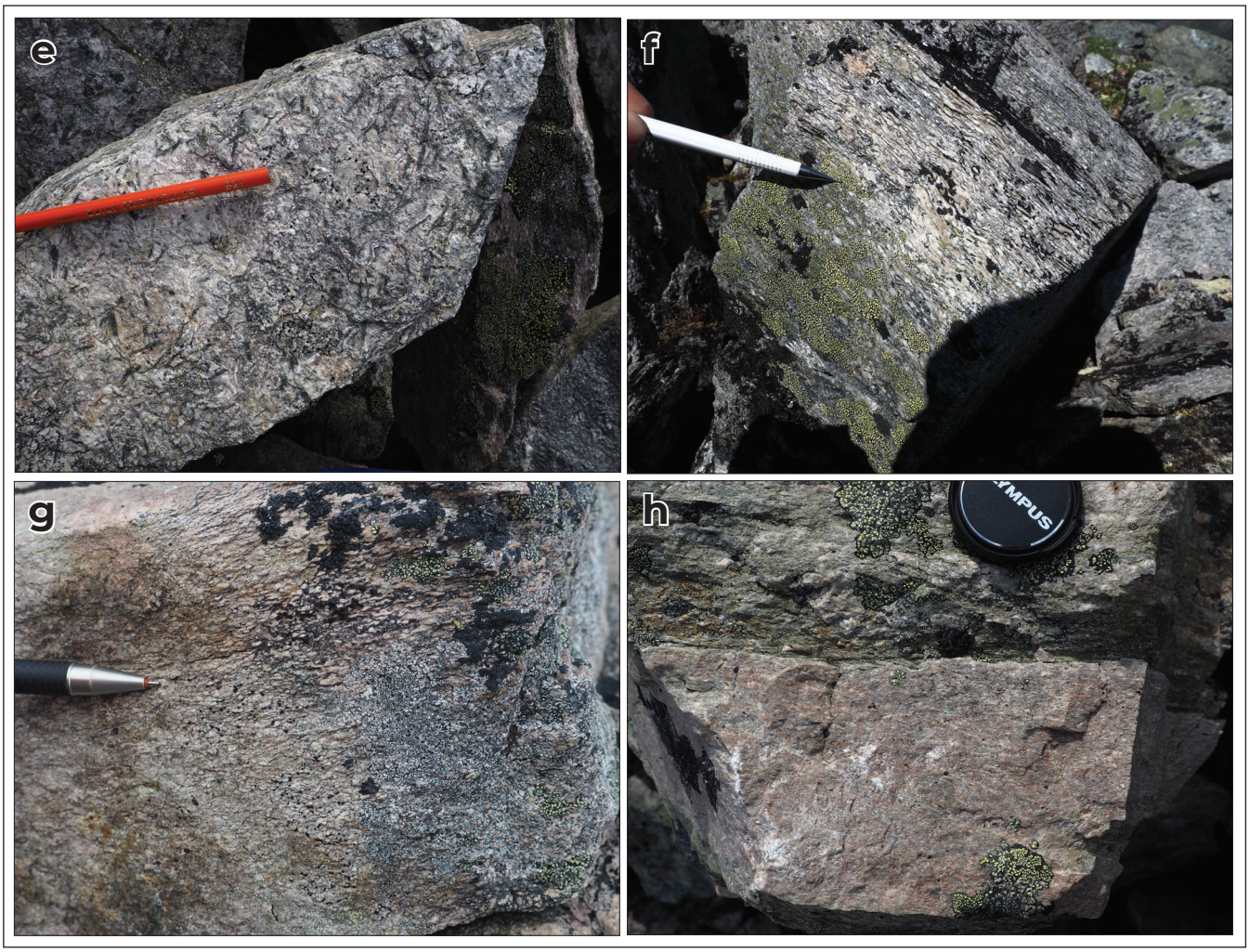

***Figure 14** continued. **(e)** Elongate pseudomorphs of hornblende in leucotonalite; pencil for scale. **(f)** Scaly weathered surface of white weathering leucotonalite; pencil for scale. **(g)** Outcrop photograph of Mississippian metagranodiorite outcrop, from which geochronology sample 20DMO-043 was obtained; pencil for scale. **(h)** Pink-weathering, epidote-rich (metagranodiorite?) dike in metatonalite; lens cap for scale.*

The rock exhibits a penetrative to semi-penetrative foliation that is defined by abundant, preferentially aligned white mica and epidote. The foliation anastomoses around ovoid, rounded crystals of twinned plagioclase. The rocks also includes polycrystalline quartz, accessory phases, and minor retrograde chlorite (Fig. 15).

A sample of this intrusion (20DMO-043; Fig. 15) was separated for U-Pb geochronology. Details on the methods used for this and other geochronology samples are included in the digital Appendix. Two zircon populations were identified in this sample. The first comprises relatively large, elongate crystals that commonly exhibit oscillatory and/or sector zoning. Some of these crystals have thin bright (CL) rims. These crystals have Eu/Eu* values in the range 0.11–0.63, ΣREE values in the range of 385–4403, (Gd/Yb)cn ratios of 0.02–0.06 and Th/U ratios of 0.26–0.91 (Appendix). Calculated Ti in zircon temperatures are in the range of 631–809°C. The second population consists of zircons that are mostly small, equidimensional crystals with complex zoning patterns. These crystals, which have very little U, very low Th/U and ΣREE, are interpreted as metamorphic crystals. It is likely that the bright (CL) rims on the igneous zircon crystals are related to this episode of metamorphic zircon growth.

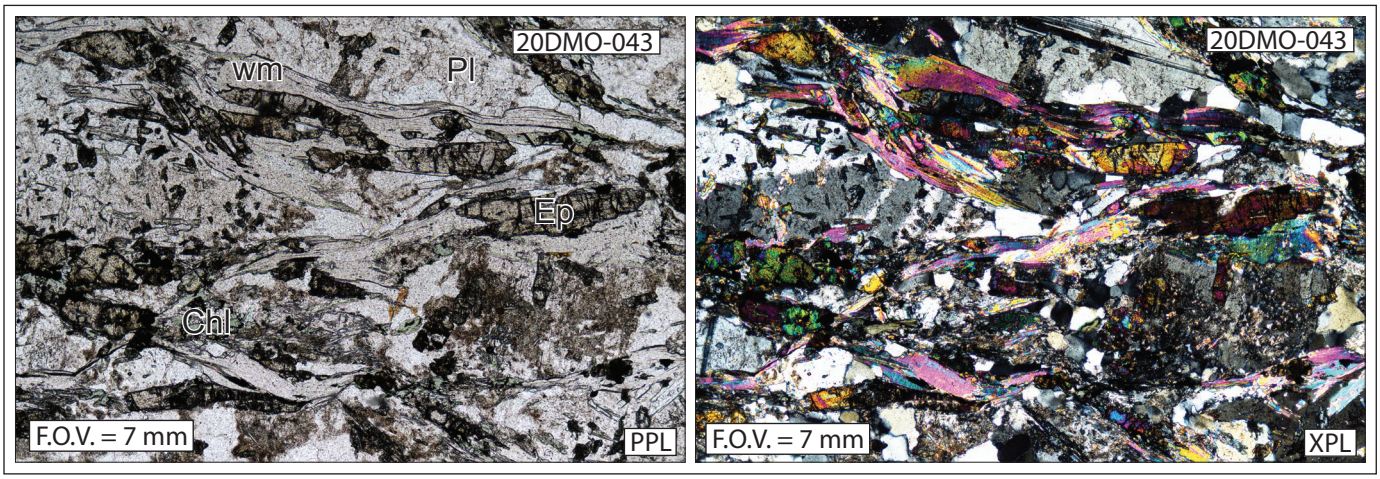

Figure 15. *Thin section photographs of metagranodiorite sample 20DMO-043. The foliation is mostly defined by abundant white mica and epidote. PPL – plane polarized light; XPL- cross-polarized light.*

The igneous population yielded a LA-ICPMS weighted mean $^{206}Pb/^{238}U$ date of 335.2 ± 4.0 Ma (MSWD = 1.5), based on 11 of the 15 analyzed spots, none of which sampled rim material (Fig. 16 a,b; Appendix). Four of these grains were selected for CA-TIMS analysis and all plot along the concordia, with a range in $^{206}Pb/^{238}U$ dates from 330.23 ± 0.24 to 336.09 ± 0.23 Ma (Fig. 16c; Table 1). The scatter in the data is attributed to incorporation of small amounts of metamorphic rim material and/or lead loss, while the oldest date is interpreted as a close approximation to the age of crystallization. This date is within the range of the Tatlmain and Kelly suites. The Tatlmain suite includes at least part of the Mt. Hazel orthogneiss, which underlies parts of the Teslin (105C), Jennings River (104O) and Atlin (104N) map areas (Mihalynuk *et al.* 2006) and crosscuts the 'Jennings Marker succession'.

Due to the extremely low levels of U present in the metamorphic crystals, only four LA-ICPMS spot analyses yielded acceptable data. The weighted mean $^{206}Pb/^{238}U$ date of the four analyses is 225 ± 16 Ma (MSWD = 2.2). Five metamorphic crystals were selected for CA-TIMS analysis. Three were single crystals while the fourth fraction included two small grains. All fractions returned similar Early Jurassic dates, and the three youngest yielded a weighted mean $^{206}Pb/^{238}U$ date of 194.76 ± 0.63 Ma (MSWD = 1.6; Fig. 16c; Table 1). This is interpreted as the age of metamorphic zircon growth.

The Livingstone pluton and Wiley succession host numerous thin (mostly centimetre to decimetre thick) dikes and plugs that appear pink and also contain abundant green epidote (Fig. 14h). These dikes could be related to the Mississippian (ca. 336 Ma) metagranodiorite of the Sawtooth Range.

Permian

Late Permian quartz augen schist

Quartz-feldspar augen schist is exposed east of the Little Bear fault, on either side of the Boswell River. A narrow band, approximately 200–400 m wide, can be traced >10 km northwestward from the boundary of the Iron Creek pluton to the slopes above the Boswell River. The band is locally discordant to lithological contacts. There is further exposure of the unit along strike, west of Falls Creek on the north side of the Boswell River. This is interpreted as a separate body on the map (Fig. 2), but it is possible that the augen schist forms a single, continuous belt. The schist is well foliated, commonly chlorite-rich, is mostly fine grained, weathers grey to green, and typically contains distinctive, commonly blue, quartz augen several mm in diameter (Fig. 17a).

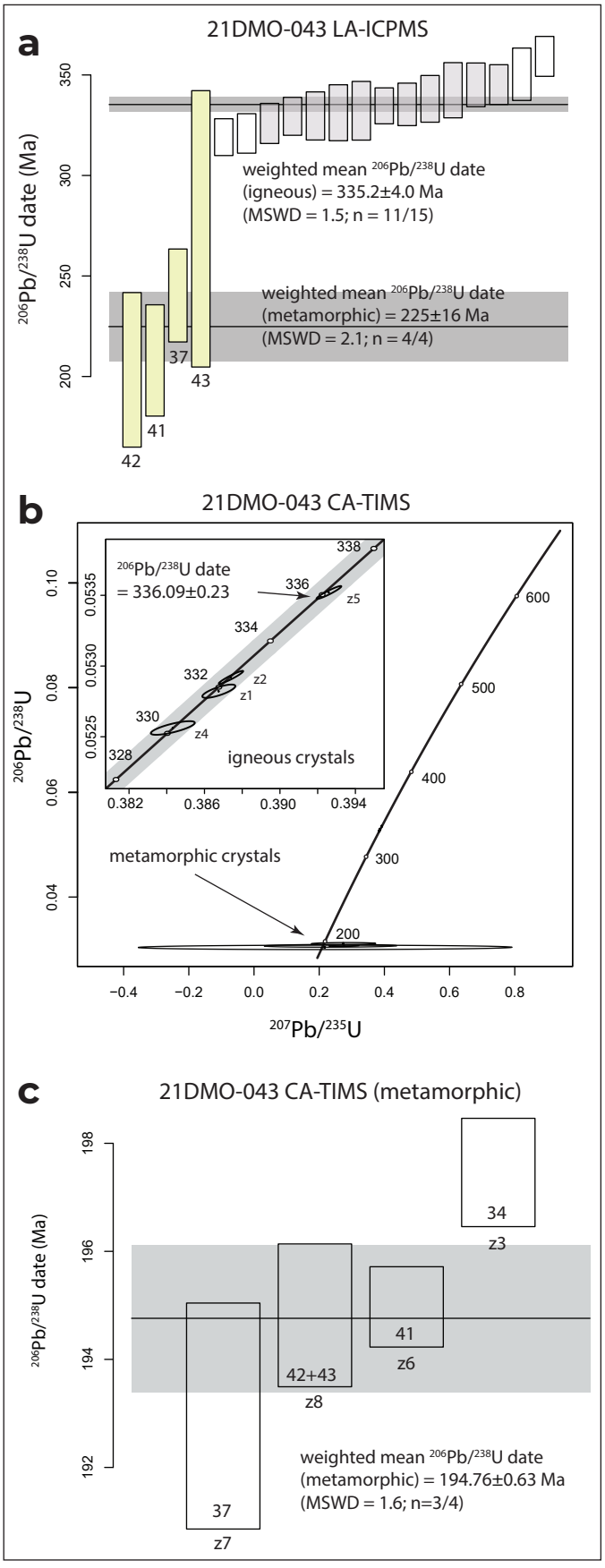

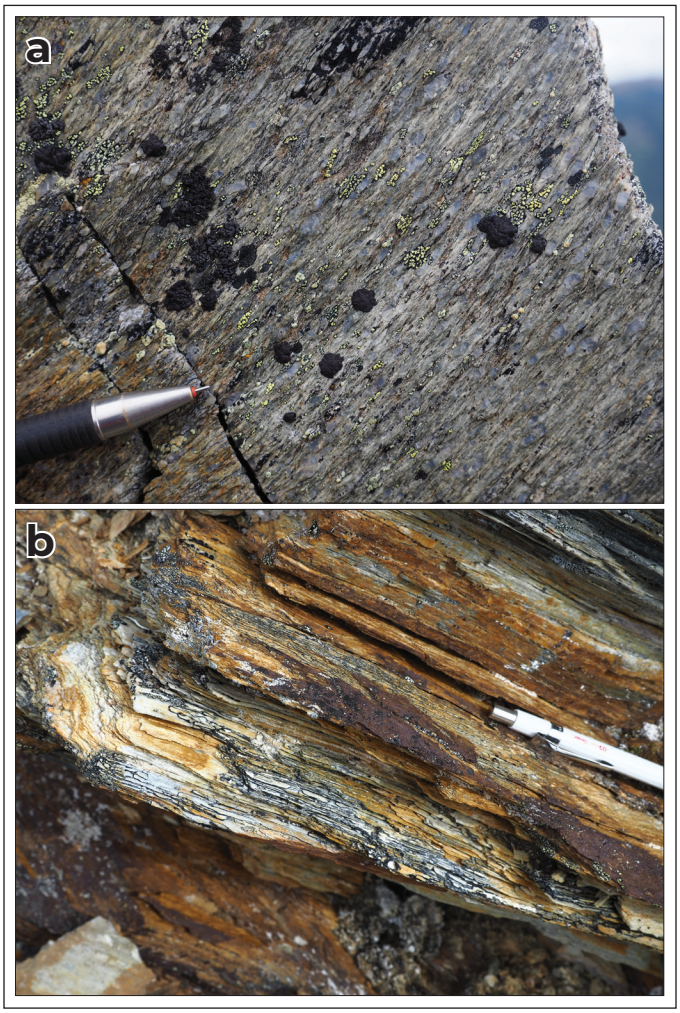

Figure 17. *Field photographs of Permian rocks.* ***(a)*** *Augen schist with abundant blue-grey quartz augen; pencil for scale.* ***(b)*** *Scaly, rusty weathering white felsic schist; pencil for scale*

Figure 16. *U-Pb geochronology results from sample 20DMO-043.* ***(a)*** *LA-ICPMS results for igneous (shaded grey/hollow fill) and metamorphic (pale yellow fill) zircon crystals. The shaded grey analyses contribute to the weighted mean date for the igneous crystals.* ***(b)*** *Results of CA-TIMS analysis of four igneous and four metamorphic crystals.* ***(c)*** *The metamorphic crystals yield a precise, Early Jurassic weighted mean $^{206}Pb/^{238}U$ date. Numbers adjacent to dates on weighted mean plots refer to LA-ICPMS spots analyses (see Appendix). Zircon crystals analyzed by CA-TIMS are labelled z1, z2 etc. (see Table 1). Images of all zircons are included in the Appendix.*

Table 1. *CA-TIMS zircon U-Pb isotopic data. Continued on next page.*

									Radiogenic Isotope Ratios							
Sample	LA-ICPMS	Th/U	$^{206}Pb^*$ x10^{-13} mol	mol % $^{206}Pb^*$	Pb* (pg)	Pb_c (pg)	Pb*/Pb_c	$^{206}Pb/^{204}Pb$	$^{208}Pb/^{206}Pb$	$^{207}Pb/^{206}Pb$	% err	$^{207}Pb/^{235}U$	% err	$^{206}Pb/^{238}U$	% err	corr. coef.
(a)	spot label	(b)	(c)	(c)	(c)	(c)	(c)	(d)	(e)	(e)	(f)	(e)	(f)	(e)	(f)	
18EB052																
z1	46	0.338	7.0377	99.97%	168.15	0.19	883	55341	0.107	0.051468	0.065	0.292984	0.129	0.041305	0.069	0.967
z2	45	0.351	13.2695	99.98%	318.20	0.17	1925	120228	0.111	0.051481	0.062	0.293062	0.127	0.041306	0.069	0.969
z4	51	0.379	4.9831	99.96%	120.38	0.18	666	41309	0.120	0.051461	0.061	0.292846	0.128	0.041291	0.069	0.985
z5	47	0.335	4.6788	99.96%	111.70	0.15	735	46131	0.106	0.051498	0.067	0.292947	0.130	0.041276	0.069	0.963
z6	52	0.497	1.9809	99.91%	49.40	0.14	349	20949	0.157	0.051442	0.077	0.292754	0.138	0.041293	0.071	0.928
20DMO043																
z5	53	0.786	1.5677	99.92%	42.11	0.11	388	21624	0.248	0.053227	0.074	0.392597	0.137	0.053520	0.070	0.950
z2	38	0.474	1.4768	99.90%	36.64	0.12	311	18813	0.150	0.053118	0.073	0.387404	0.137	0.052920	0.071	0.956
z1	39	0.406	1.1740	99.61%	28.61	0.38	75	4600	0.128	0.053128	0.137	0.386760	0.185	0.052822	0.073	0.769
z4	35	0.380	0.3144	99.51%	7.61	0.13	59	3673	0.120	0.053053	0.197	0.384321	0.248	0.052562	0.075	0.757
z3	34	0.120	0.0083	86.08%	0.19	0.11	2	130	0.038	0.064017	29.418	0.274431	29.482	0.031105	0.526	0.131
z6	37	0.057	0.0115	88.96%	0.26	0.12	2	163	0.018	0.065278	13.533	0.276257	13.609	0.030707	0.395	0.206
z8	42 + 43	0.000	0.0065	81.32%	0.14	0.12	1	97	0.000	0.055476	70.831	0.234584	70.903	0.030682	0.703	0.107
z7	41	0.027	0.0037	76.05%	0.08	0.10	1	75	0.009	0.052032	215.151	0.217879	215.200	0.030384	1.123	0.046
20DMO070B																
z1	60	0.308	1.3675	99.87%	32.44	0.15	223	14104	0.098	0.052870	0.079	0.308412	0.143	0.042327	0.073	0.934
z2	59	0.353	1.5732	99.87%	37.74	0.17	225	14072	0.112	0.051540	0.081	0.294976	0.142	0.041528	0.070	0.936
z3	56	0.351	1.3390	99.89%	32.11	0.13	254	15909	0.111	0.051534	0.078	0.294811	0.140	0.041509	0.069	0.946
z4	61	0.450	1.5988	99.88%	39.38	0.15	256	15600	0.143	0.051550	0.077	0.295006	0.139	0.041523	0.069	0.946
z5	89	0.373	0.9333	99.36%	22.52	0.50	45	2810	0.118	0.051578	0.193	0.294943	0.238	0.041493	0.073	0.719
z6	65	0.325	0.9304	99.73%	22.15	0.21	105	6637	0.103	0.051594	0.120	0.295461	0.173	0.041552	0.073	0.828
20DMO124A																
z2	200	0.760	2.8706	99.94%	76.56	0.15	496	27844	0.241	0.051180	0.067	0.274385	0.131	0.038901	0.069	0.965
z3	197	0.896	2.4781	99.93%	68.31	0.15	458	24921	0.284	0.051139	0.071	0.274169	0.134	0.038901	0.069	0.953
z4	202	0.511	1.6997	99.90%	42.54	0.14	311	18629	0.162	0.051184	0.078	0.274295	0.139	0.038884	0.069	0.937
z1	194	0.485	4.6130	99.96%	114.67	0.15	747	45017	0.154	0.051122	0.069	0.273956	0.131	0.038883	0.070	0.945
z5	204	0.673	4.5777	99.96%	119.46	0.15	806	46250	0.213	0.051166	0.064	0.274140	0.129	0.038876	0.070	0.964
z6	212	0.869	1.9348	99.87%	52.99	0.20	262	14361	0.276	0.051142	0.077	0.273991	0.139	0.038873	0.069	0.947

(a) z1, z2, *etc.* are labels for analyses composed of single zircon grains that were annealed and chemically abraded (Mattinson, 2005).

(b) Model Th/U ratio calculated from radiogenic $^{208}Pb/^{206}Pb$ ratio and $^{207}Pb/^{235}U$ date.

(c) Pb* and Pbc are radiogenic and common Pb, respectively. mol % $^{206}Pb^*$ is with respect to radiogenic and blank Pb.

(d) Measured ratio corrected for spike and fractionation only. Fractionation correction for analyses done with tracer solution BSU1B is 0.16 ± 0.03 (1 sigma) %/amu (atomic mass unit) for single-collector Daly analyses, based on analysis of EARTHTIME ^{202}Pb-^{205}Pb ET2535 tracer solution. Fractionation correction for analyses done with tracer solution ET2535 is based on measurement of $^{202}Pb/^{205}Pb$ in the tracer solution.

(e) Corrected for fractionation and spike. Common Pb in zircon analyses is assigned to procedural blank with composition of $^{206}Pb/^{204}Pb$ = 18.04 ± 0.61%; $^{207}Pb/^{204}Pb$ = 15.54 ± 0.52%; $^{208}Pb/^{204}Pb$ = 37.69 ± 0.63% (1 sigma). $^{206}Pb/^{238}U$ and $^{207}Pb/^{206}Pb$ ratios corrected for initial disequilibrium in $^{230}Th/^{238}U$ using a D(Th/U) of 0.20 ± 0.05 (1 sigma).

(f) Errors are 2 sigma, propagated using algorithms of Schmitz and Schoene (2007) and Crowley et al. (2007).

(g) Calculations based on the decay constants of Jaffey et al. (1971). $^{206}Pb/^{238}U$ and $^{207}Pb/^{206}Pb$ dates corrected for initial disequilibrium in $^{230}Th/^{238}U$ using a D(Th/U) of 0.20 ± 0.05 (1 sigma).

***Table 1** continued. CA-TIMS zircon U-Pb isotopic data.*

		Isotopic Dates							
Sample	LA-ICPMS	$^{207}Pb/^{206}Pb$	±	$^{207}Pb/^{235}U$	±	$^{206}Pb/^{238}U$	±	include in weighted mean?	
(a)	spot label	(g)	(f)	(g)	(f)	(g)	(f)		***Weighted Mean Calculations***
18EB052									
z1	46	260.83	1.49	260.91	0.30	260.91	0.18	x	$^{206}Pb/^{238}U$ ± random (+tracer) [+decay constant] **260.85 ± 0.08** (0.15) [0.31] MSWD = 0.7 pof = 0.57 n = 5
z2	45	261.38	1.42	260.97	0.29	260.92	0.18	x	
z4	51	260.52	1.41	260.80	0.29	260.83	0.18	x	
z5	47	262.14	1.54	260.88	0.30	260.74	0.18	x	
z6	52	259.66	1.77	260.73	0.32	260.84	0.18	x	
20DMO043									
z5	53	337.45	1.68	336.26	0.39	336.09	0.23		$^{206}Pb/^{238}U$ ± random (+tracer) [+decay constant] **194.76 ± 0.63** (0.63) [0.67] MSWD = 1.6 pof = 0.20 n = 3
z2	38	332.82	1.65	332.47	0.39	332.42	0.23		
z1	39	333.23	3.10	332.00	0.52	331.82	0.24		
z4	35	330.06	4.47	330.21	0.70	330.23	0.24		
z3	34	741.23	622.16	246.23	64.46	197.46	1.02		
z6	37	782.37	284.31	247.68	29.91	194.97	0.76	x	
z8	42 + 43	430.47	1578.34	213.98	136.80	194.82	1.35	x	
z7	41	285.77	4918.46	200.14	390.92	192.95	2.14	x	
20DMO070B									
z1	60	322.21	1.80	272.95	0.34	267.24	0.19		$^{206}Pb/^{238}U$ ± random (+tracer) [+decay constant] **262.25 ± 0.08** (0.11) [0.30] MSWD = 2.2 pof = 0.07 n = 5
z2	59	264.00	1.86	262.47	0.33	262.30	0.18	x	
z3	56	263.74	1.79	262.34	0.32	262.18	0.18	x	
z4	61	264.48	1.77	262.49	0.32	262.27	0.18	x	
z5	89	265.70	4.42	262.44	0.55	262.08	0.19	x	
z6	65	266.44	2.75	262.85	0.40	262.45	0.19	x	
20DMO124A									
z2	200	247.90	1.55	246.19	0.29	246.02	0.17	x	$^{206}Pb/^{238}U$ ± random (+tracer) [+decay constant] **245.93 ± 0.07** (0.10) [0.28] MSWD = 0.8 pof = 0.58 n = 6
z3	197	246.08	1.64	246.02	0.29	246.01	0.17	x	
z4	202	248.10	1.80	246.12	0.30	245.91	0.17	x	
z1	194	245.31	1.60	245.85	0.29	245.91	0.17	x	
z5	204	247.30	1.48	246.00	0.28	245.86	0.17	x	
z6	212	246.20	1.77	245.88	0.30	245.85	0.17	x	

(a) z1, z2, etc. are labels for analyses composed of single zircon grains that were annealed and chemically abraded (Mattinson, 2005).

(b) Model Th/U ratio calculated from radiogenic $^{208}Pb/^{206}Pb$ ratio and $^{207}Pb/^{235}U$ date.

(c) Pb* and Pbc are radiogenic and common Pb, respectively. mol % $^{206}Pb^*$ is with respect to radiogenic and blank Pb

(d) Measured ratio corrected for spike and fractionation only. Fractionation correction for analyses done with tracer solution BSU1B is 0.16 ± 0.03 (1 sigma) %/amu (atomic mass unit) for single-collector Daly analyses, based on analysis of EARTHTIME ^{202}Pb-^{205}Pb ET2535 tracer solution. Fractionation correction for analyses done with tracer solution ET2535 is based on measurement of $^{202}Pb/^{205}Pb$ in the tracer solution

(e) Corrected for fractionation and spike. Common Pb in zircon analyses is assigned to procedural blank with composition of $^{206}Pb/^{204}Pb$ = 18.04 ± 0.61%; $^{207}Pb/^{204}Pb$ = 15.54 ± 0.52%; $^{208}Pb/^{204}Pb$ = 37.69 ± 0.63% (1 sigma). $^{206}Pb/^{238}U$ and $^{207}Pb/^{206}Pb$ ratios corrected for initial disequilibrium in $^{230}Th/^{238}U$ using a D(Th/U) of 0.20 ± 0.05 (1 sigma).

(f) Errors are 2 sigma, propagated using algorithms of Schmitz and Schoene (2007) and Crowley et al. (2007).

(g) Calculations based on the decay constants of Jaffey et al. (1971). $^{206}Pb/^{238}U$ and $^{207}Pb/^{206}Pb$ dates corrected for initial disequilibrium in $^{230}Th/^{238}U$ using a D(Th/U) of 0.20 ± 0.05 (1 sigma).

The rock is locally sulphide-rich and in these areas is rusty weathering. Compositional banding is also locally apparent. The quartz augen are round and are variably strained/recrystallized. Although quartz augen are characteristic they are not ubiquitous; some rocks contain plagioclase phenocrysts in addition to, or instead of quartz, and non-porphyritic varieties are locally developed. Northeast of the Red Mountain deposit, the unit includes a thin interval of coarser grained, bright green weathering, chloritic, non-porphyritic schist (metatonalite). The matrix of the quartz augen schist is typically composed of recrystallized quartz, plagioclase, epidote, chlorite and white mica. Locally, flakes of biotite are also developed. The augen schist could represent a shallow level subvolcanic intrusion; alternatively, its apparent crosscutting nature could be a result of extrusion onto an unconformable surface.

A sample of dacitic quartz augen schist was selected for geochronology (20DMO-70B; Fig. 18). Zircon crystals are faceted and columnar (Appendix). Many exhibit oscillatory zoning, while some crystals include more complex, patchy CL characteristics. LA-ICPMS analysis was carried out on 54 crystals (Fig. 19a). Forty-one analyses contribute to a weighted mean $^{206}Pb/^{238}U$ date of 263.7 ± 2.1 Ma (MSWD = 1.2; Fig. 19b). Six crystals were selected for analysis by CA-TIMS (Fig. 19c). Five of these give equivalent results, with a weighted mean $^{206}Pb/^{238}U$ date of 262.25 ± 0.08 Ma (MSWD = 2.2; Table 1). This is interpreted as the crystallization age of the rock. The sixth zircon crystal produced an older ($^{206}Pb/^{238}U$), discordant date.

Late Permian felsic schist

A number of thin (1 m to several metres thick) bands of rusty weathering fine-grained felsic schist were encountered on either side of the Little Bear fault. The schist is white on fresh surfaces (Fig. 17b). It is scaly and friable, typically breaking along rusty brown to yellow (limonitic) foliation planes. Small quartz phenocrysts are locally visible. The boundaries of these felsic schist bands are generally parallel to the foliation/compositional banding, but they are interpreted as small deformed intrusions (sills/dikes), based on their scattered occurrence in contact with a variety of other rock types, some of which are demonstrably older.

A sample of this rock type (18EB-052) was collected by E. Bordet in 2018 from the lower part of the Rosy succession and separated for U-Pb geochronology. The zircon crystals are faceted, and exhibit fine oscillatory zoning in CL (Appendix). Thirteen LA-ICPMS spots were analyzed on 11 grains (Fig. 20a). The weighted mean $^{206}Pb/^{238}U$ date for all thirteen spots is 251.4 ± 2.1 Ma. Five crystals were selected for CA-TIMS dating, and these yielded equivalent dates, with a weighted mean $^{206}Pb/^{238}U$ date of 260.85±0.08 Ma (MSWD = 0.7; Fig. 20b,c; Table 1). This is interpreted as the crystallization age of the rock. A ca. 260 Ma date was reported by Colpron et *al.* (2017) from a similar felsic schist in the southern Livingstone Creek area (105E/8).

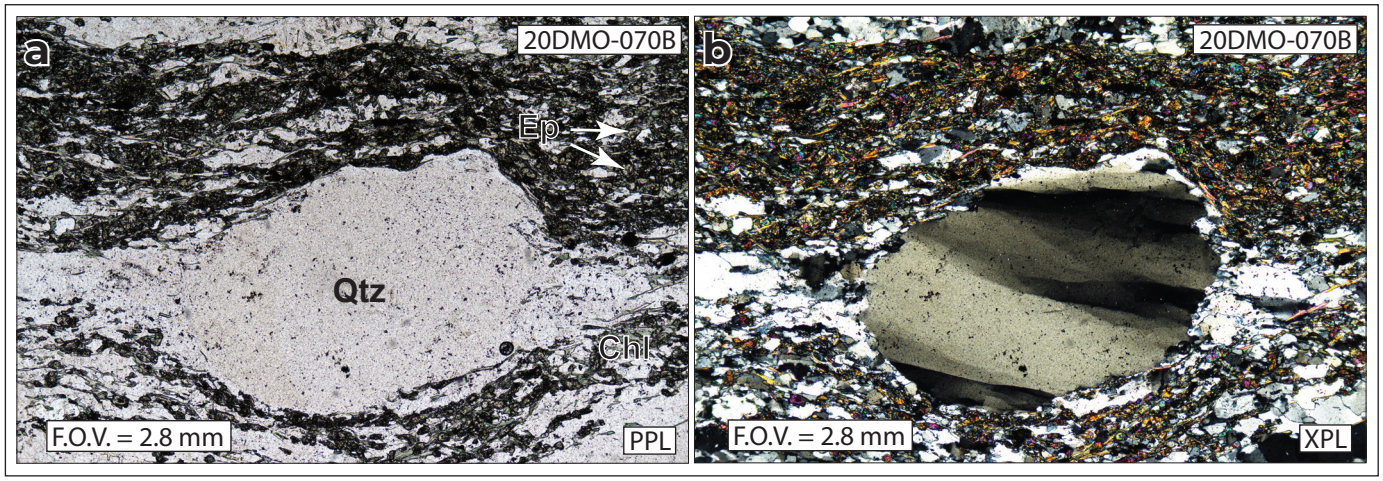

Figure 18. *Photomicrographs of strained quartz augen in geochronology sample 20DMO-070B. The matrix of the rock includes fine grained crystals of epidote, chlorite, quartz and plagioclase (a) PPL; (b) XPL.*

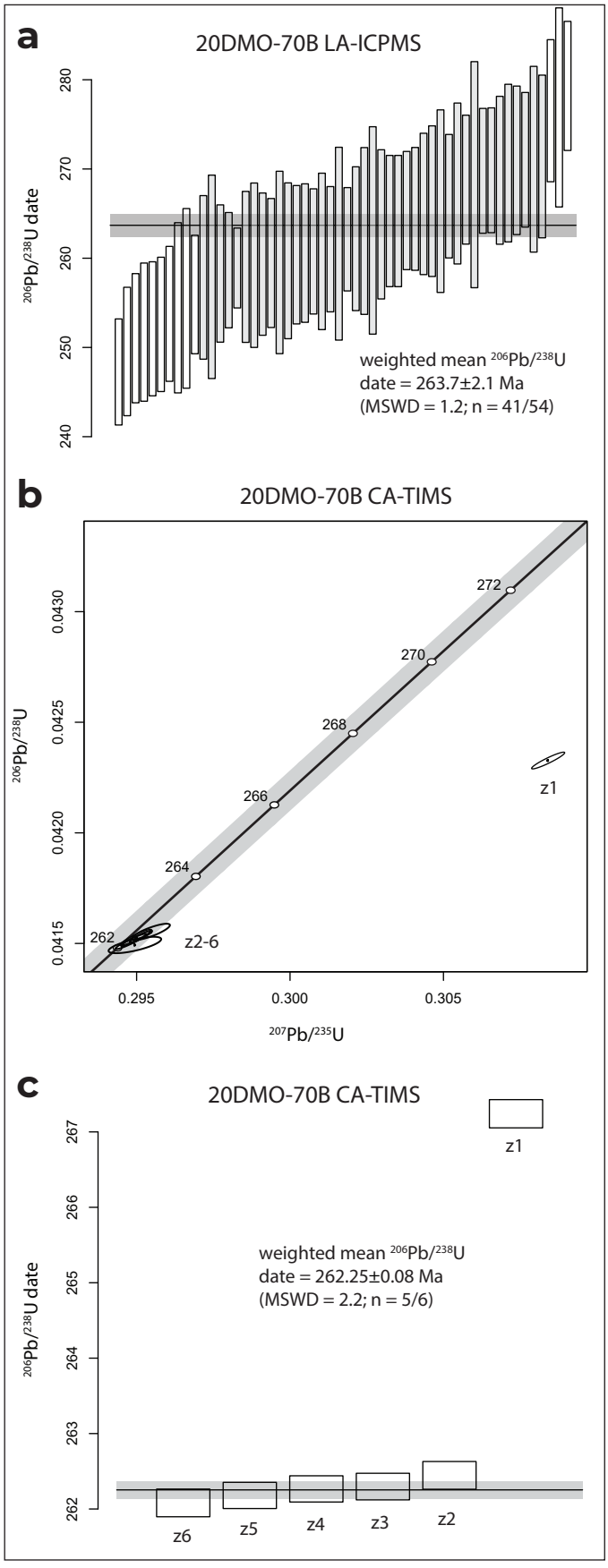

Middle Triassic

Rosy Lake metagabbro

A small (~6 km^2) body of foliated metagabbro or metadiorite is exposed on the west flank of the Sawtooth Range. This metagabbro, which was first recognized by Stevens (1994) coincides with an aeromagnetic high (Kiss and Boulanger, 2018). It is interpreted to intrude rocks on the west side of the Sidney Creek fault and is crosscut by the Early Jurassic Sawtooth stock (Fig. 2). The rock is generally medium to coarse-grained. It is generally well foliated (Fig. 21a), but parts of it are only weakly foliated (Fig. 21b). The metagabbro is dominated by interlocking regions of pseudomorphed plagioclase (mostly clinozoisite) and black (locally dark green) regions, which are clusters of green amphibole that are interpreted to have replaced igneous pyroxene (Fig. 22). The rock also contains quartz, magnetite, biotite and other accessory phases; biotite is restricted to secondary clusters around magnetite. The foliation in and around the intrusion is commonly at a high angle to the regional trend and is folded at the outcrop scale. The metagabbro is intruded by anastomosing weakly deformed, white, sugary textured leucocratic quartz-feldspar dikes and by dikes of porphyritic hornblende-bearing granodiorite.

A sample of coarse-grained, foliated gabbro (20DMO-124A; Fig. 22) was selected for U-Pb geochronology. Zircon from this rock is stubby to elongate and is faceted. It exhibits concentric oscillatory zoning, and in some cases, sector zoning (Appendix).

Figure 19. *U-Pb geochronology results for augen schist sample 20DMO-070B.* ***(a)*** *LA-ICPMS results from 54 spot analyses. CA-TIMS results are presented in* ***(b)*** *and* ***(c)****. Five of the six zircons contribute to the 262.25 ± 0.08 Ma weighted mean $^{206}U/^{238}Pb$ date. Zircon crystals analyzed by CA-TIMS are labelled z1, z2 etc. (see Table 1). Images of all zircons are included in the Appendix.*

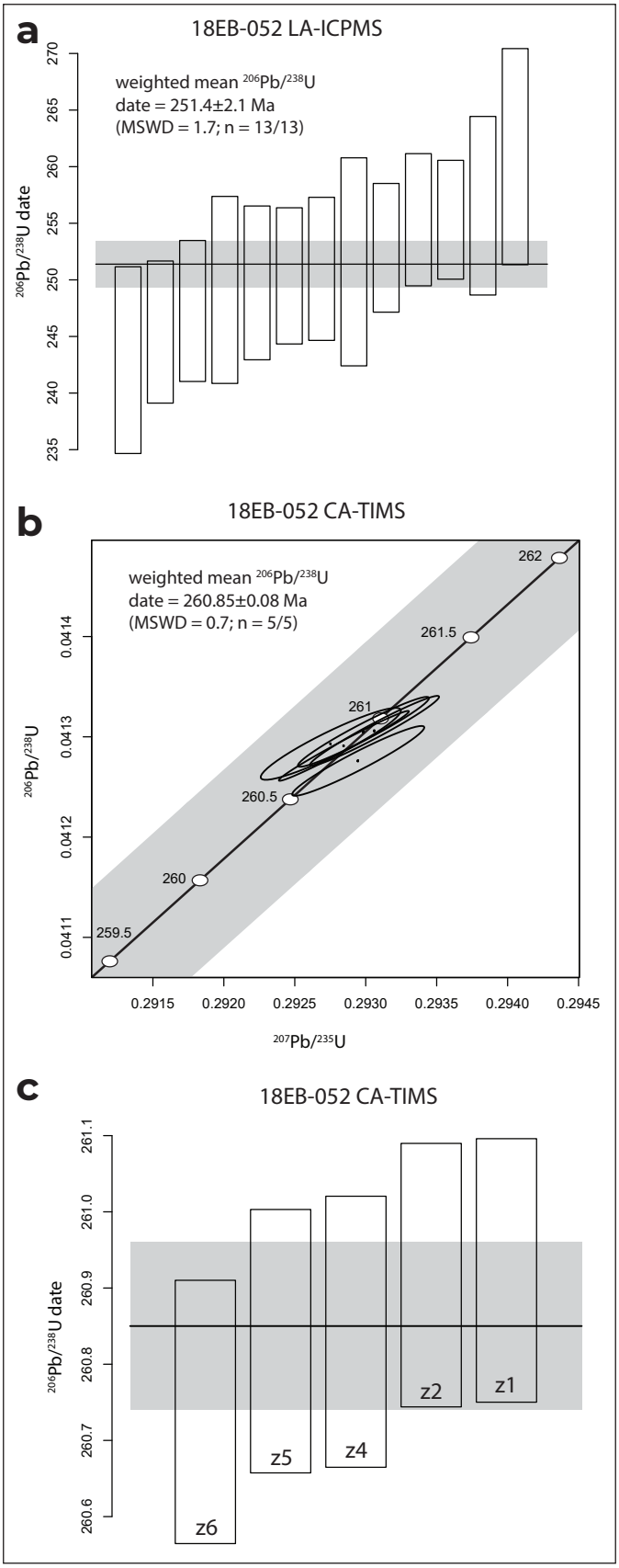

Figure 20. *U-Pb zircon geochronology results from 18EB-052.* **(a)** *LA-ICPMS results from 18EB-052. CA-TIMS results are plotted on Concordia* **(b)** *and weighted mean* **(c)** *diagrams. Zircon crystals analyzed by CA-TIMS are labelled z1, z2 etc. (see Table 1). Images of all zircons are included in the Appendix.*

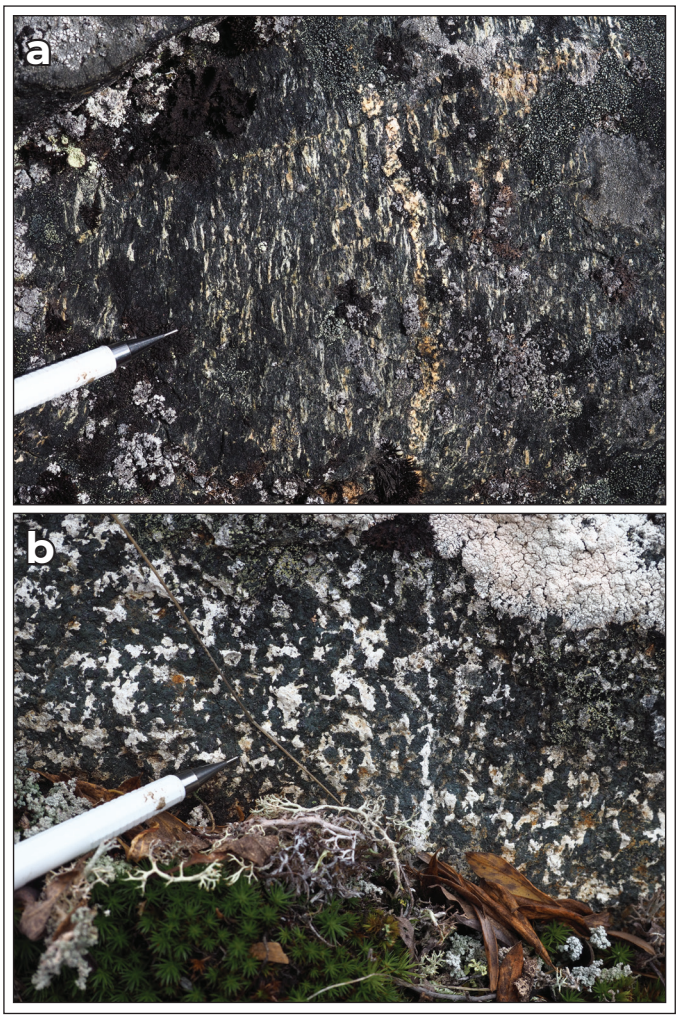

Figure 21. *Field photographs of Middle Triassic metagabbro. Most of the intrusion is well foliated* **(a)**, *but some relatively weakly enclaves are preserved* **(b)**. *Pencil for scale.*

Thirty-six LA-ICPMS spot analyses revealed a single population, and thirty of these spots contribute to the weighted mean $^{206}Pb/^{238}U$ LA-ICPMS date of 243.1 ± 2.0 Ma (MSWD = 1.07; Fig. 23a; Appendix). Six grains were selected for analysis by CA-TIMS, and all six produced equivalent results with a weighted mean $^{206}Pb/^{238}U$ date of 245.93 ± 0.07 Ma (MSWD = 0.8; Fig. 23c; Table 1). This is interpreted as the crystallization age of the metagabbro.

The crystallization age of the Rosy Lake metagabbro is the same as that of zircon that was recovered

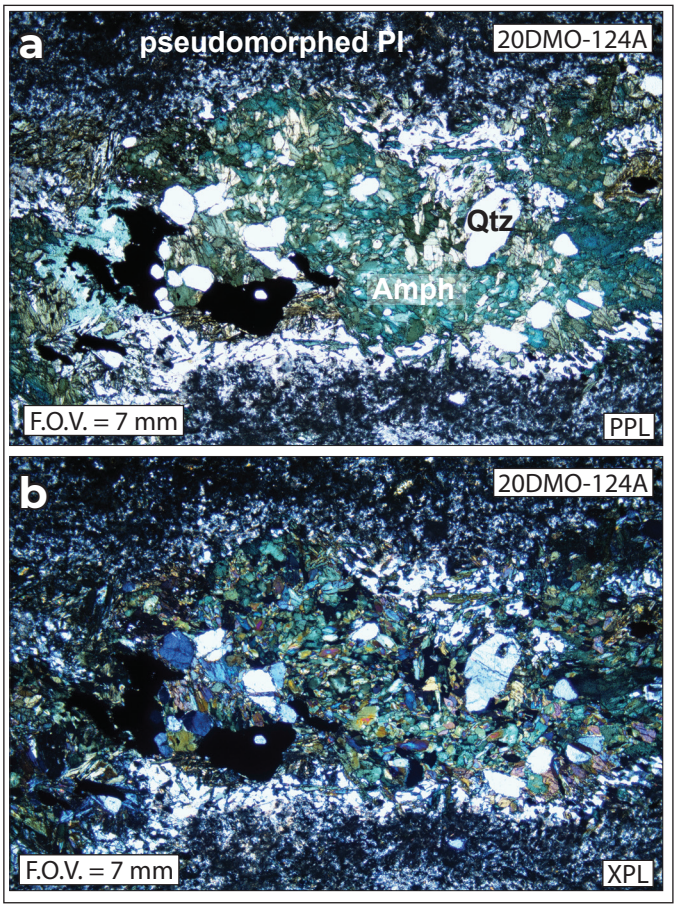

Figure 22. *Photomicrographs of U-Pb geochronology metagabbro sample 20DMO-124,* ***(a)*** *plane polarized (PPL) and* ***(b)*** *cross-polarized (XPL). Amphibole clusters are interpreted as pseudomorphs of igneous pyroxene crystals.*

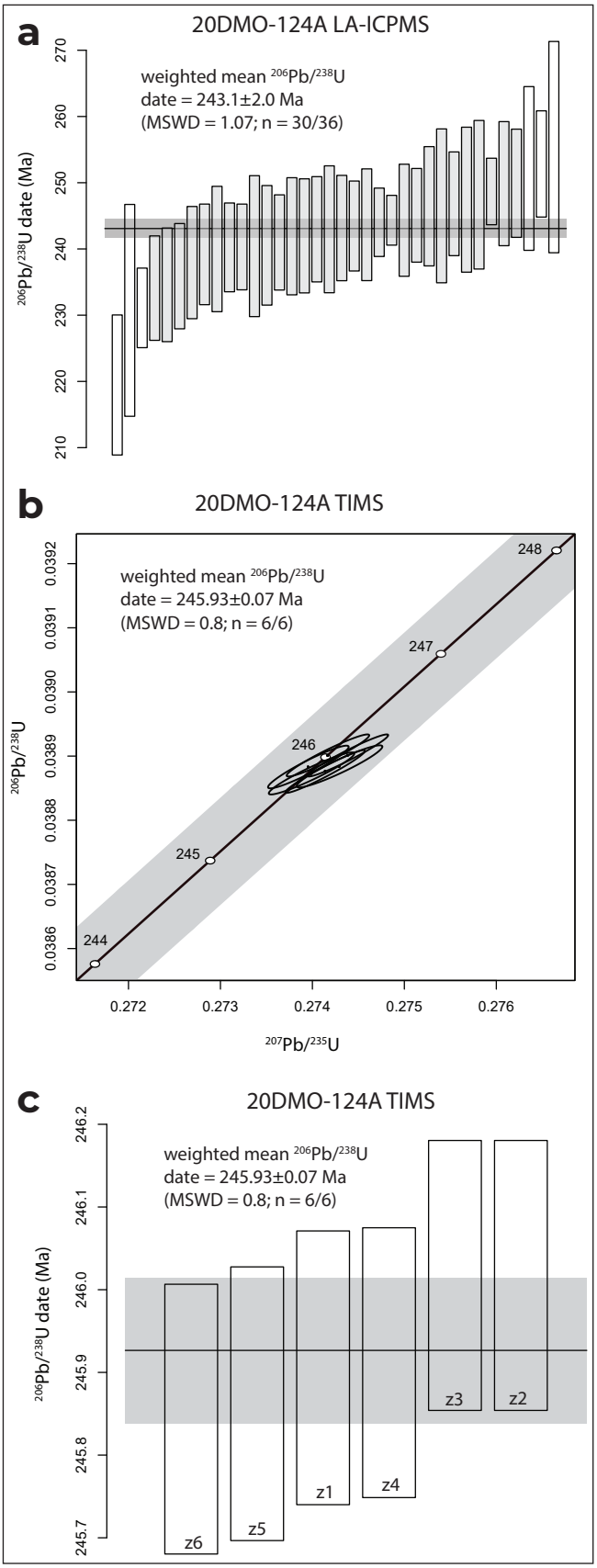

Figure 23. *U-Pb data from 20DMO-124A.* ***(a)*** *LA-ICPMS data derived from single spots analyses on 36 crystals. CA-ID-TIMS results are illustrated in* ***(b)*** *and* ***(c)****. All six crystals that were analyzed overlap to produce a tightly constrained weighted mean Middle Triassic date. Zircon crystals analyzed by CA-TIMS are labelled z1,z2 etc. (see Table 1). Images of all zircons are included in the Appendix.*

from volcaniclastic rocks of the Michie formation (244.64 ± 0.08 Ma; 245.85 ± 0.07 Ma; Bickerton *et al.* 2020), and also overlaps with the age of the Streak Mountain peridotite (245.4 ± 0.8 Ma; Gordey *et al.* 1998). These are located southwest of the Teslin fault in part of the northern Cordillera that has traditionally been referred to as Cache Creek terrane, but recently assigned to the Atlin terrane (Zagorevski *et al.* 2021). A near identical age (244.71 ± 0.09 Ma) was reported by Bordet et al., (2019) from arc rocks of the Joe Mountain formation, which is exposed at a similar latitude to the study area on the west side of the Teslin fault. Middle Triassic gabbro/diorite and arc volcanic rocks also form part of the Tsaybahe Group, which is in stratigraphic contact with the Paleozoic Stikine assemblage and Late Triassic volcanic rocks of the Stikine terrane (Stuhini Group) in the Stikine Canyon-Dease Lake area of northern British Columbia (Read, 1983; van Straten and Wearmouth, 2019).

Lokken suite (EJL)

The Sawtooth stock crosscuts the Sidney Creek fault in the western part of the map area. It is composed of equigranular Hb-Bt granodiorite, monzodiorite, quartz diorite and hornblendite (Stevens, 1994; Sack *et al.* 2020). A central region is dominated by intermediate varieties (Fig. 24a), while parts of the margin are more mafic (Fig. 24b). Textural evidence suggests incorporation and partial dissolution of the marginal mafic phases by granodiorite (Fig. 24 c,d).

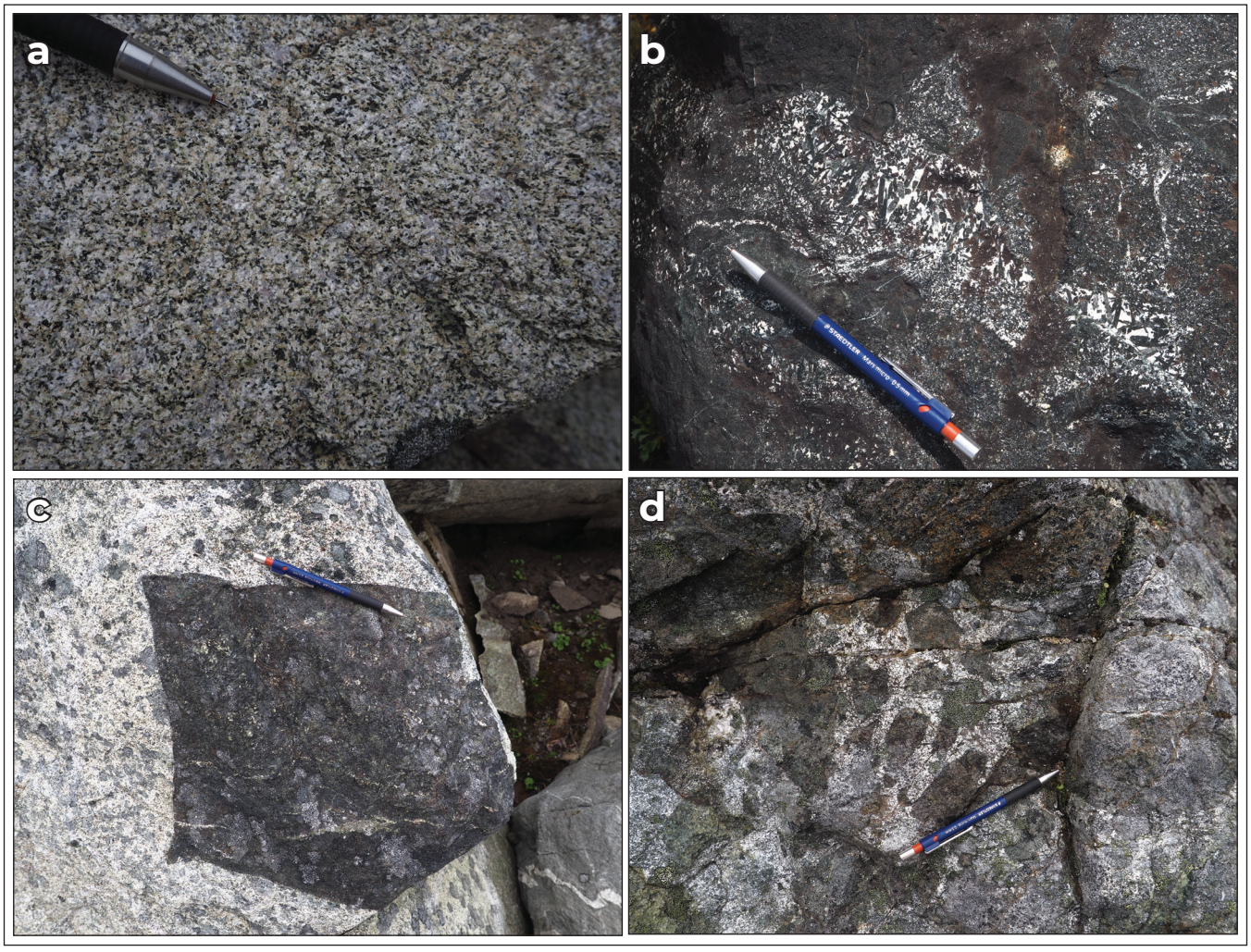

Figure 24. *Sawtooth stock field photographs.* ***(a)*** *Equigranular hornblende-bearing granodiorite from the relatively felsic, central part of the intrusion.* ***(b)*** *Black hornblendite with pegmatitic hornblende-plagioclase enclaves; pencil for scale. Angular* ***(c)*** *to rounded* ***(d)*** *xenoliths of hornblendite are included in the granodioritic phase of the stock.*

The Sawtooth stock forms part of the Lokken suite (Sack *et al.*, 2020), a characteristic feature of which is the presence of clinopyroxene cores inside hornblende crystals. Stevens (1994) reported a U-Pb titanite date of 193.2 ± 4.2 Ma from quartz-diorite to hornblendite of the Sawtooth stock, while Sack *et al.* (2020) produced a zircon U-Pb CA-TIMS date of 184.28 ± 0.07 Ma from monzodiorite of the same body.

Satellite intrusions of the Sawtooth stock include a small, lozenge-shaped body, composed of coarse equigranular granodiorite to diorite that crosscuts the Flat Creek succession southeast of the Sawtooth stock, and small hornblendite intrusions on its northern flank. Hornblendite is black to green, and is dominated by densely intergrown amphibole crystals several mm to 2 cm long, with interstitial plagioclase.

The Loon Lake stock intrudes the quartzite unit of the Slate Mountain succession north of Indian River. The northern part of the pluton is mostly equigranular granodiorite to diorite with local hornblendite, while the southern part is more felsic (granodiorite) and mildly porphyritic, with slender 5–7 mm amphibole crystals and K-feldspar phenocrysts.

The Rosy and Gunsight successions are intruded by a pair of narrow elongate intrusions composed of coarse-grained hornblendite and hornblende-biotite pegmatite southeast of the Sawtooth pluton (Fig. 25 a,b). Hornblendite locally includes small lenses/veins of quartz and epidote. These intrusions crosscut the dominant foliation in the area, but minor post-crystallization deformation/hydration is indicated by kinking of some biotite aggregates (Fig. 25b) and chloritization of hornblende. Some outcrops near the margin of the body include patches of unfoliated hornblende diorite. These localized patches have highly irregular boundaries with the hornblendite, and include numerous angular to rounded (partially digested) hornblendite inclusions (xenoliths).

Both hornblende and biotite from this intrusion yielded Early Jurassic K-Ar dates (ca. 188–185 Ma; Hunt and Roddick, 1992). Hornblendite and minor gabbro also form another small intrusion in the Swift River pluton southeast of the Red Mountain access road.

Small (centimetres to metres thick), hornblende-bearing, dacitic or andesitic dikes are common in parts of the Sawtooth Range. These dikes typically crosscut the penetrative foliation and are generally undeformed or weakly deformed. Varieties include dikes with abundant delicate acicular hornblende crystals in a white weathering dacitic/andesitic matrix (Fig. 25c), dikes with densely arranged, blocky plagioclase crystals in a fine-grained matrix (Fig. 25d) and porphyritic dikes with cm-scale K-feldspar crystals in a fine, hornblende-bearing matrix (Fig. 25e).

Green dikes and xenolithic dikes

Forest green dikes dominated by matted chlorite crystals intrude part of the Swift River pluton in the southern part of the area. The dikes form swarms, range from several cm to >1 m thick and crosscut the penetrative foliation. Many are homogeneous, but some are rich in xenoliths. The xenoliths are mostly angular clasts of the country rock (foliated metatonalite). A similar xenolithic dike or diatreme, approximately 20 m in diameter, was observed in the Livingstone pluton; here the foliated clasts form a clast-supported array, and the chlorite-rich dike-rock is restricted to angular gaps between clasts (Fig. 25f). Locally, patches of coarse-grained, unfoliated intermediate-mafic rocks along the margins of some clasts suggest melting and formation of modified magma during intrusion of the dike.

There are no direct age estimates for the green/xenolithic dikes but they are the same relative age as the pegmatitic hornblendite of the Sawtooth Range; it is possible that they represent fine-grained equivalents and form part of the Lokken suite, or alternatively could form part of a younger magmatic suite.

Felsic dikes and pegmatite

White, coarse-grained, deformed pegmatite forms foliation-parallel sheets and pods in several locations near the eastern boundary of the Livingstone Creek pluton. The sheets are generally centimetres to >1 m thick, and contain abundant folia of country rock. Colpron *et al.* (2017) reported a Middle Triassic U-Pb zircon date (243 ± 1.5 Ma) from deformed pegmatite along strike to the North in the Livingstone Creek area, but no data exist for examples in the study area.

Figure 25. *Minor Jurassic intrusions field photographs.* ***(a)*** *Pegmatitic hornblendite that intrudes the Gunsight succession; lens cap for scale.* ***(b)*** *The hornblendite includes cm-scale, kinked biotite crystal aggregated; pencil for scale.* ***(c)*** *Xenolith-rich, hornblende-bearing dacitic dike, interpreted as part of the Lokken suite; pencil for scale.* ***(d)*** *Thin crowded, hornblende-bearing, plagioclase porphyritic dike that crosscuts deformed metagabbro of the Sawtooth succession. Pencil-sized eraser for scale.* ***(e)*** *Porphyritic granodiorite dike in the Rosy Lake metagabbro; pencil for scale.* ***(f)*** *Xenolith-rich intrusion/breccia that is dominated by rotated clasts of metatonalite with spaces filled by fine-grained, dark green, chlorite-rich intrusive rock; lens cap for scale.*

Garnet amphibolite on the eastern margin of the Livingstone Creek pluton, and similar rocks southwest of the Sidney Creek fault commonly contain thin (millimetres to centimetres thick), foliation-parallel felsic to intermediate (plagioclase-rich) layers. These are commonly lensoidal or anastomosing, weather white to green and in some cases contain sparse amphibole. An outcrop of amphibolite/garnet amphibolite adjacent to the Red Mountain road contains numerous leucocratic layers that exhibit a variety of relationships to the dominant foliation. The least deformed/most highly crosscutting parts of these intrusions grade into white weathering felsic pegmatite.

Deformed, homogeneous felsic dikes crosscut metagabbro of the Sawtooth succession north of Sidney Creek Lakes. These are white (fresh), white weathering and equigranular.

Weakly deformed, porphyritic hornblende-bearing dikes (Lokken suite) that crosscut the Rosy Lake metagabbro are themselves cut by white to pale pink weathering aplite. Curved apophyses and deflection of the foliation along its margins indicates that their emplacement overlapped with the final stages of penetrative deformation.

Cretaceous

Quiet Lake batholith and Iron Creek stock

The Quiet Lake batholith occupies much of the eastern fringe of the study area. The southwestern part of the batholith comprises coarse-grained porphyritic biotite and granitic pegmatite. Biotite granite is porphyritic and commonly crowded, with abundant cm-scale cream to pink K-feldspar crystals, grey to black smoky quartz, biotite books and white plagioclase (Fig. 26a). In places, a weak foliation/preferred alignment is discernable. Pegmatite contains pink K-feldspar and the same mineralogy as the granite. Biotite-muscovite granite forms marginal phases near the southern part of the d'Abbadie fault (Figs. 2 and 26b). U-Pb zircon dates from the Quiet Lake batholith are ca. 100–114 Ma but there are no data from the study area.

The Iron Creek stock is coincident with a circular aeromagnetic anomaly (Kiss and Boulanger, 2018) and may be separate from the main Quiet Lake batholith. The parts that were examined are lithologically distinct from the Quiet Lake batholith, being dominated by white weathering muscovite-biotite granite, leucogranite aplite and pegmatite. There are no geochronological constraints on the age of the Iron Creek stock but a Cretaceous age is likely based on its composition, lack of penetrative deformation, and low-pressure contact metamorphic aureole (see below).

Granitic orthogneiss of the Grass Lakes suite is intruded by undeformed to weakly deformed, medium-grained, pale yellow weathering, equigranular biotite granite and aplite (e.g., Fig. 13a). This does not resemble rocks observed in the Quite Lake batholith and may instead be part of the Late Cretaceous (ca. 103–96 Ma) Seagull suite that intrudes the d'Abbadie fault zone farther north (e.g., Colpron *et al.* 2017).

Red Mountain intrusions and porphyry deposit

A distinctive set of dikes are concentrated around the Red Mountain deposit (Fig. 26c), but are found throughout the area, from the Wiley succession east of the Livingstone pluton to the Swift River pluton. These dikes of rhyolite/dacite are cream-yellow, fine grained and porphyritic, with phenocrysts of rounded quartz and/or plagioclase, typically ~1 mm in diameter (Fig. 26d). Flow-banding textures are locally developed (Fig. 26e). The dikes are blocky, resistant, and often have pyrolusite-coated surfaces. Two main sets of dike are developed in the vicinity of the Red Mountain porphyry deposit: 1) a set that strikes northwest-southeast, parallel to the regional strike, and 2) a set that strikes approximately north-south.

The Red Mountain porphyry deposit is located approximately 2 km northeast of the Little Bear fault (Fig. 2). It is surrounded by a spectacular zone of red-weathering pyritic hornfels (Fig. 26c) that was first reported by Lees (1936). The deposit is primarily hosted in quartz monzonite that intruded graphitic phyllite of the Slate Mountain succession. Several overlapping intrusive phases and breccias have been identified, including a post-mineralization, pyritic quartz-eye diorite that is also exposed at surface (Brown and Kahlert, 1986). The mineralization is concentrated at depth and consists of fine-grained selvages and

disseminations within thin quartz veins that cut the quartz monzonite and hornfels. The calculated reserve is 187 270 000 tonnes grading 0.167% MoS_2 (Brown and Kahlert, 1986). Existing K-Ar data suggest the Red Mountain deposit formed in the Late Cretaceous (*ca.* 81–87 Ma; Yukon Geological Survey geochronology database), but new U-Pb and Re-O dating is underway to establish an accurate date. The age and style of the Red Mountain deposit appear to be similar to the Adanak Mo porphyry (Smith and Arehart, 2010) near Atlin, British Columbia.

Other minor Cretaceous intrusions

Volumetrically minor, small (centimetres to ~2 m thick), undeformed dikes are scattered sporadically through the area. Varieties include: green, non-vesicular porphyritic dacitic dikes with prominent mica (phlogopite?) and plagioclase phenocrysts (Fig. 26f); green (fresh), beige-brown weathering, feather-textured dacite dikes with sparsely distributed quartz eyes and cream, partially filled amygdules; brown weathering, vesicular dikes with abundant phlogopite(?) crystals, and equigranular biotite monzonite with felted texture. A larger (1 km long) porphyritic dacite(?) plug straddles the southwestern boundary of the Quiet Lake batholith north of the Boswell River.

Deformation and metamorphism

The study area is located in a region characterized by mostly steeply-dipping planar structures, which has previously been referred to as the Teslin suture zone (Tempelman-Kluit, 1979), or Teslin tectonic zone (Stevens *et al.*, 1995). This elongate, strike-parallel zone was interpreted as a subduction/imbricate complex by Tempelman-Kluit (1979) and Hansen (1989, 1992) but more detailed work led to recognition of coherent stratigraphy (Stevens *et al.*, 1995) and regional scale folds (Gallagher, 1999; de Keijzer *et al.*, 1999).

The results described here support the contention that, rather than represent a melange or imbricate zone (as initially proposed by Tempelman-Kluit, 1979), the area is underlain by coherent, albeit highly deformed stratigraphic successions that have experienced several generations of folding. Three main phases of folding are recognized, and the general geometry and sequence of deformation observed in the study area is comparable to that described by de Keijzer *et al.* (1999) in the Last Peak area to the north.

Folds and penetrative structures

Pre-Jurassic metavolcanic and metasedimentary rocks of the area are penetratively deformed and tightly folded. The fold axial planes and their axial planar foliation(s) are mostly steeply or moderately steeply dipping and fold axial traces are approximately parallel to the overall trend of the orogen. There is a small but a systematic change in the orientation of structures from NNW-SSE north of Indian River, to NW-SE around the Boswell River and areas to the southeast (Fig. 2).

Map-scale folding is responsible for interdigitation of the Wiley and Slate Mountain successions in the northern part of the area, and of component parts of the Sawtooth succession along strike to the southeast. Map-scale folds are well developed in the Sawtooth Range, where they are defined by marker carbonate of the Rosy succession, and by folding of the metabasalt/metagabbro contact. Map-scale folds were not documented southwest of the Sidney Creek fault, an area that is dominated by the Swift River pluton.

Most outcrops contain evidence for two or three phases of deformation (Figs. 27 and 28). Typically, the cleavage along which rocks break most easily is a second generation, spaced to penetrative foliation (S_2; Fig. 27a) that overprints an earlier, penetrative foliation. The early foliation (S_1) is almost invariably parallel to compositional layering and the axial plane of rare F_1 folds. In regions where S_2 is most intensely developed, S_1 may not be discernable (except around some fold hinges) and layering is transposed. F_2 folds are close to isoclinal (Fig. 27b), and are responsible for folding and reorientation of early intersection (L^1_0) and mineral lineations on S_1 (Fig. 27c). The S_2 foliation is axial planar to the map scale folds described above. The foliation (S_2) and fold axial planes are mostly steeply dipping, but lineation orientations are more variable. Stretching lineations developed in metatonalite are mostly moderately steeply to steeply pitching, while intersection lineations in layered rocks range from shallow to steeply pitching.

Figure 26. *Field photographs of Cretaceous intrusions.* **(a)** *Coarse-grained biotite granite of the Quiet Lake batholith includes cm-scale K-feldspar phenocrysts; pencil for scale.* **(b)** *Foliated pegmatite along the eastern strand of the d'Abbadie fault south of Fish Creek; lens cap for scale.* **(c)** *Red and yellow gossan surrounds the Red Mountain Mo porphyry deposit, which is hosted in rocks of the Slate Mountain succession, south of the Boswell River. The elevation difference between the valley floor and the top of the gossanous hill is approximately 400 m.* **(d)** *Sulphide-rich, porphyritic rhyolite of the Red Mountain suite. Small (1–2 mm) plagioclase phenocrysts are visible in the fine-grained matrix.* **(e)** *Banded texture formed by elongated filled vesicles in rhyolite of the Red Mountain suite.* **(f)** *Pale brown phlogopite(?) and plagioclase crystals form phenocrysts in a green, fine-grained dacite dike. Pencil tip for scale.*

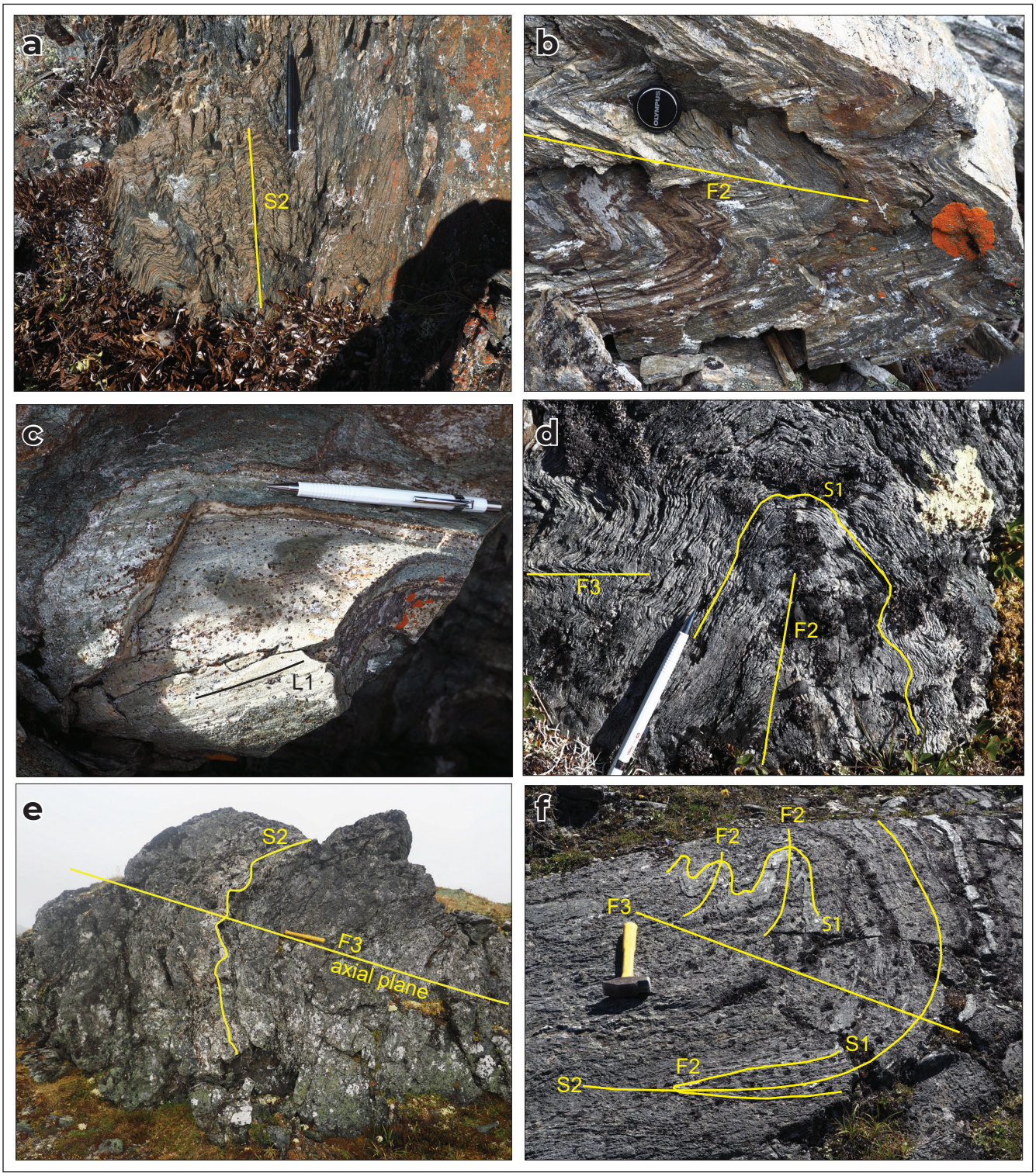

Figure 27. *Fold and deformation styles.* ***(a)*** *Chevron folding of micaceous quartzite; lens cap for scale.* ***(b)*** *Spaced S_2 cleavage at high angle to S_0/S_1 in metasandstone with abundant phyllitic partings; pencil for scale.* ***(c)*** *Polished surface of deformed metatonalite showing reorientation of D_1/$_2$ structures across the trace of an F_3 fold; hammer for scale.* ***(d)*** *Tight F_2 fold whose limbs are overprinted by F_3 chevron folds/crenulations; pencil for scale.* ***(e)*** *Outcrop scale F_3 fold with shallow-dipping axial plane; central Sawtooth Range; hammer for scale.* ***(f)*** *L_1 intersection lineations folded around the axis of a F_2 fold; pencil for scale.*

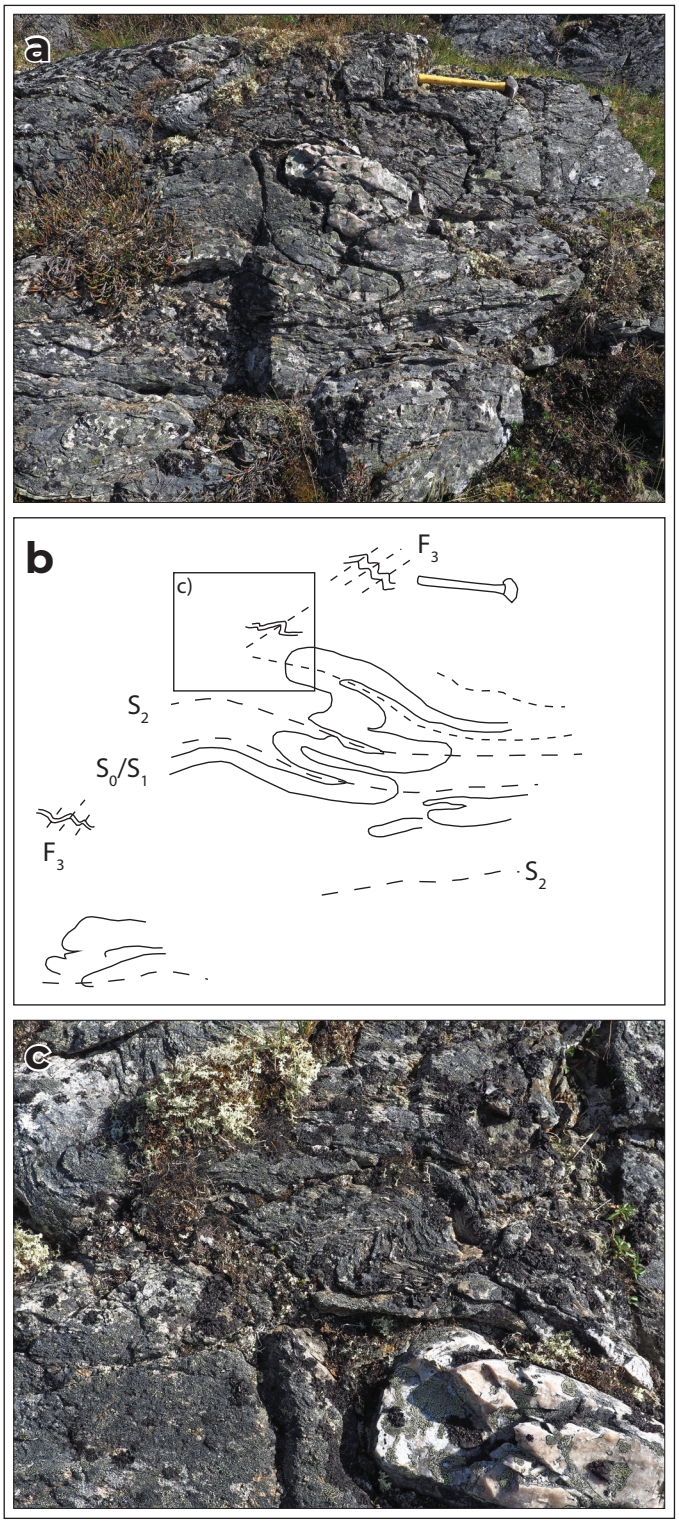

Figure 28. *Photographs and sketch of polyphase structures in an outcrop of metatonalite (Swift River pluton).* ***(a)*** *and* ***(b)*** *are images of the entire outcrop, while* ***(c)*** *is a close-up photographs of the regions marked on* ***(b)****.*

In parts of the area, S_2 and earlier structures are overprinted by another phase of widespread folding (F_3; Figs. 27d–f and 28). These structures are particularly well developed in the western part of the Sawtooth Range and in parts of the Swift River pluton (Fig. 28a–c), and are less conspicuous in the northeastern part of the map area. Chevron folds and crenulations (F_3) are widely developed at a variety of scales from mm to cm-scale crinkles and crenulations to map scale folds. These are open to tight, but only locally exhibit an axial planar cleavage. Axial planes of F_3 folds generally dip at shallow to moderate angles, have mostly shallow to moderate-plunging axes, and are responsible for widespread reorientation of earlier structures. The shallow dip of the lithological enveloping surface immediately northwest of the Sawtooth stock is attributed to its position on the shallow limb of an F_3 fold (Fig. 29).

Major Faults

Little Bear fault

The Little Bear fault separates mafic volcanic and plutonic rocks of the Sawtooth succession from metasedimentary units of the Slate Mountain succession (Fig. 2). It runs approximately parallel to the Boswell River valley in the central part of the map area. To the southeast, it crosses low vegetated spurs and, in the vicinity of the Iron Creek stock, higher mountain ridges. The fault is plugged by the Iron Creek stock (Fig. 30a).

The area around the southwestern flank of the Iron Creek stock is well exposed and the fault is located to within a few metres (the contact is covered by talus), between outcrops of 1) hornfelsed (contact metamorphosed) graphitic phyllite and 2) a thin sliver of calc-schist (Rosy succession) in contact with skarn-altered metabasalt (Sawtooth succession). The orientation of foliations and lineations in rocks on either side of the fault is similar to elsewhere in the surrounding area, and no evidence for high intensity brittle deformation was observed near the fault. Similar observations were made northwest of the Iron Creek stock where the Little Bear fault bifurcates around a lozenge of

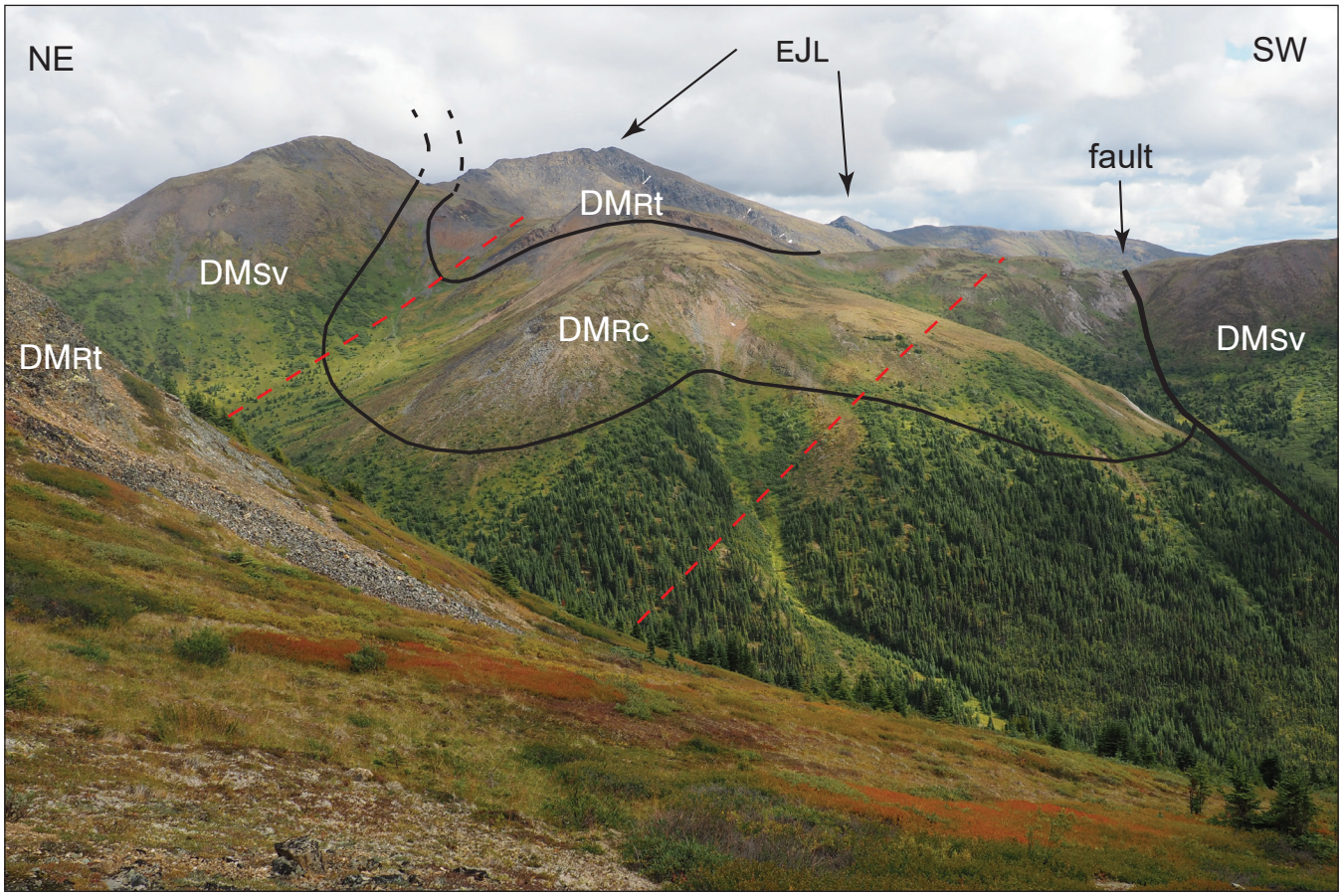

Figure 29. *Shallow-dipping, folded panel of Sawtooth and Rosy successions on the west flank of the Sawtooth Range. The overall shallow dip of the units contrasts with most of the area and is interpreted to reflect its position on the flat limb of a large F_3 fold. The cross-strike distance between the fold axial traces (dashed red lines) is approximately 1 km.*

Rosy succession/Gunsight succession and crosses two gullies. Penetratively deformed metabasalt of the Sawtooth succession that is in fault contact with the Rosy succession has a finely banded, stripy appearance, and lacks evidence for significant brittle deformation. These observations suggest that juxtaposition of units across the Little Bear fault preceded or accompanied the regional deformation and epidote-amphibolite facies metamorphism.

Sidney Creek fault

The Sidney Creek fault separates metavolcanic and metasedimentary rocks of the Gunsight and Rosy successions from the Flat Creek succession. A fault contact is supported by juxtaposition of different units along its trace and the metamorphic contrast between garnet amphibolite of the Flat Creek succession and greenschist-facies metavolcanic rocks on its northeastern side. Exposures of the fault were not encountered but it is interpreted to be folded and have variable, but mostly steep dip, based on the geometry of its trace. Shallow-dipping foliation in the Gunsight succession changes to subvertical adjacent to the fault, with identical strike. The Sidney Creek fault is crosscut by the Early Jurassic Sawtooth stock. The fault is interpreted to emerge on the NW side of the stock, where it may form part of the margin of the Rosy Lake metagabbro (Fig. 2).

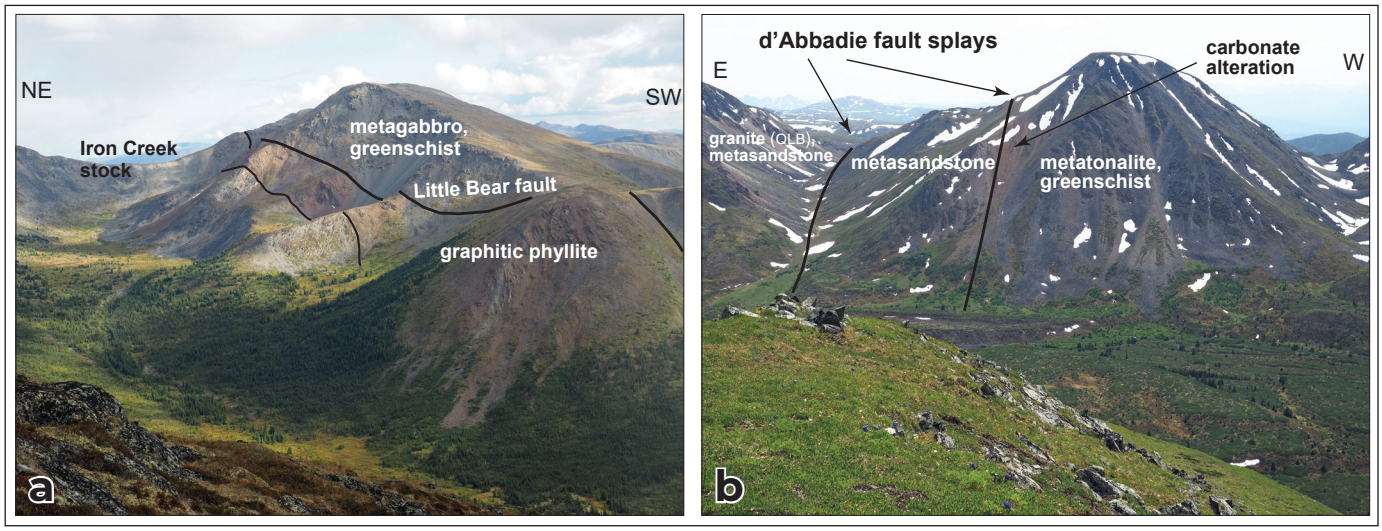

Figure 30. *Landscape photographs of the Little Bear and d'Abbadie faults.* ***(a)*** *The Little Bear fault, which separates graphitic phyllite/argillite (Slate Mountain succession) from metagabbro and greenschist of the Sawtooth succession is plugged by the Iron Creek stock. The distance from the spur in the right foreground to the peak in the centre is approximately 1.6 km.* ***(b)*** *View across Fish Creek, towards two splays of the d'Abbadie fault. The western splay is marked by a zone of orange talus due to carbonate alteration along the fault. The eastern splay occupies the valley and is coincident with subvertical layering/foliation in quartzite and granitic rocks.*

D'Abbadie fault

The d'Abbadie fault is a north-south striking steep fault/shear zone that crosscuts the regional trend and has clear geophysical expression on aeromagnetic maps of the region (Gallagher, 1999; Colpron et *al.*, 2017). The fault zone includes steep brittle structures that are superimposed on a zone of mylonite, which formed during dextral shearing. The mylonite is largely restricted to the immediate vicinity of elongate Late Cretaceous granitic intrusions that are parallel to the trace of the fault zone. Harvey et *al.* (1997) estimated dextral offset of approximately 4 km across the d'Abbadie fault, while a larger offset was inferred by Gabrielse et *al.* (2006), who interpreted the d'Abbadie fault as a splay of the Teslin fault.

The d'Abbadie fault extends into the northern part of the study area. Two main splays cross the ridges on either side of Fish Creek, and bound an orange weathering zone of abundant brittle deformation and pervasive carbonate alteration (Fig. 30b). The faults are steeply dipping, layering in metasandstone is steeply dipping and granite/pegmatite within this zone has a steeply dipping foliation. This brittle deformation is superimposed on a wider region of penetrative strain. Outcrops of Grass Lakes suite orthogneiss adjacent to the eastern strand of the d'Abbadie fault on the western flanks of Mount Black are affected by shear bands (S-C' fabrics) that indicate dextral shearing. These die out to the east over the course of several hundred metres and the rock transitions to deformed orthogneiss with mostly symmetrical strain shadows on phenocrysts, which lacks significant arrays of shear bands. Mineral elongation lineations pitch steeply in the region affected by dextral shear bands and beyond, and therefore appear to predate formation of the shear bands. Splays of the d'Abbadie fault are interpreted to extend across Indian River, but die out before meeting the Boswell River. An eastern splay is in contact with the Quiet Lake batholith; the granite contains abundant scaly fractures and coarse muscovite. Subvertical "sills" of garnet-bearing pegmatite along the trace of this fault are also foliated (Fig. 26b).

The change in the orientation of regional structures from NW-SW to ~N-S around the Indian River is coincident with the tip zone of the d'Abbadie fault and is interpreted to result from late, fault-related deflection of structures towards parallelism with the fault zone.

Metamorphism

Most of the area was affected by epidote amphibolite-facies regional metamorphism during D_1-$_2$ deformation. This resulted in crystallization of chlorite, epidote, plagioclase series feldspar and green amphibole in metabasic rocks, and conversion of mudstone rich in organic material to graphitic phyllite. Many fine-grained metabasites were thoroughly recrystallized, but some coarse-grained rocks, such as metagabbro of the Sawtooth succession, retain their igneous texture and were pseudomorphed by metamorphic minerals (e.g., clinozoisite after plagioclase and green amphibole after pyroxene).

Slightly higher grade metamorphism affected the area southwest of the Sidney Creek fault, and at least part of the area in/around the Livingstone pluton. In these areas, metabasite is black rather than green, lacks chlorite, and amphibolite commonly contains garnet in addition to amphibole, white mica, quartz and accessory minerals. Garnet is sporadically developed in micaceous quartzite of the Flat Creek succession, and also forms part of schistose rocks within the Swift River and Livingstone plutons (Fig. 31a).

Hansen (1992) studied regional metamorphism in the area immediately north of the study area and obtained a wide spread of intermediate to high-pressure, moderate temperature estimates based on amphibole chemistry and application of a number of thermobarometers to metaplutonic, metavolcanic and metasedimentary rocks.

The age of metamorphic recrystallization of the Rosy succession is indicated by the $^{206}Pb/^{238}U$ date of 194.76 ± 0.63Ma from zircon rims on metagranodiorite in the Sawtooth Range. Hansen *et al.* (1991) also obtained Early Jurassic $^{40}Ar/^{39}Ar$ dates from the Livingstone pluton and adjacent schists. The Early Jurassic date is similar to the age of regional metamorphism in other parts of the Yukon-Tanana terrane (Berman *et al.* 2007; Clarke, 2017; Gaidies *et al.*, 2020).

Contact metamorphism of the graphitic phyllite unit (Slate Mountain succession) around the margin of the Iron Creek stock produced cordierite and andalusite-bearing hornfels, which indicates emplacement at low pressure (approximately 3.5–4 Kbar; Pattison and Vogl, 2005; Fig. 31b). Green, garnet-bearing calc-silicate adjacent to the Quiet Lake batholith is also interpreted to have formed during contact metamorphism.

Figure 31. (a) *Regional metamorphic garnet schist derived from metatonalite of the Swift River pluton; pencil for scale.* ***(b)*** *Slender pale pink andalusite crystals in graphitic metapelite adjacent to the Iron Creek pluton; pencil tip for scale.*

Discussion

Are the Slate Mountain and Flat Creek successions the same?

The Slate Mountain and Flat Creek successions contain similar rock types and are each pre-Early Mississippian. However, most of the shared rock types (graphitic phyllite, quartzite, metabasalt) are common throughout Yukon-Tanana terrane and are not diagnostic of specific rock assemblages. The most distinctive unit in the Slate Mountain succession – the green chloritic calc-schist/calc-silicate has not been recognized in the Flat Creek succession; however, only relatively small regions of the succession are preserved around the fringes of the Swift River pluton, and the boundary between the quartzite and phyllite units has not yet been observed. The garnet-bearing amphibolite of the Flat Creek succession is texturally dissimilar to banded greenschist of the Wiley succession, but is similar to thin layers of garnet amphibolite in the Mount Black area, and may be analogous to a larger garnet amphibolite body in the Slate Mountain succession east of the Livingstone pluton (Colpron, 2006; Colpron *et al.* 2017). Whatever their original stratigraphic relationships, the Slate Mountain and Flat Creek successions host similar to indistinguishable (based on field observations) metaplutonic rocks.

Significance of the Little Bear and Sidney Creek faults?

The Little Bear and Sidney Creek faults each separate rocks that are interpreted to form part of the Semenof block from those of the Yukon-Tanana terrane. The Sidney Creek fault is no younger than Early Jurassic as it is crosscut by the Sawtoooth stock. The Little Bear fault is crosscut by the Cretaceous(?) Iron Creek stock but as this pluton is undated this constraint is not definitive. The Little Bear fault lacks evidence for extensive brittle deformation and appears to have been active during or before greenschist to epidote-amphibolite-facies metamorphism and deformation; an Early Jurassic or older age is therefore likely. The Little Bear and Sidney Creek faults converge towards the eastern boundary of the area, but the nature of their interaction is unresolved. Given the apparent stratigraphic similarities and common plutonic rocks on either side of the central panel, it is possible that the Little Bear and Sidney Creek faults are parts of a single, folded detachment. This could be analogous to the Needlerock thrust of the Glenlyon area, which is a Triassic-Jurassic structure (Colpron *et al*., 2003) that marks the boundary between Yukon-Tanana terrane and the Semenof block, is associated with penetrative strain of surrounding units and lacks evidence for extensive brittle deformation.

Termination of the d'Abbadie fault

Continuity of the Slate Mountain succession across southern strands of the d'Abbadie fault suggests it accounts for little discrete offset in this area. The fault is interpreted to terminate in the northern part of the map area, with residual displacement transferred to 1) multiple splays that are associated with brittle deformation and alteration, but which accommodate relatively minor discrete offsets, and 2) deflection of regional structures into a north-south orientation around its tip zone. This interpretation is incompatible with the hypothesis (Gabrielse *et al*., 2006) that the d'Abbadie fault is a splay of the Teslin fault.

Relationship of Rosy Lake metagabbro to coeval arc successions?

The age of the Rosy Lake metagabbro is identical to that of primitive arc successions in southern Yukon and northern/central British Columbia. Bordet *et al*., (2019) suggested the Joe Mountain and Michie formations of southern Yukon, along with the Kutcho and Sitlika assemblages of British Columbia, represented parts of a primitive intra-oceanic arc that subsequently amalgamated with Cache Creek terrane. Zagorevski *et al.* (2021) included Middle Triassic arc rocks (Joe Mountain Formation, Michie formation, Kutcho assemblage, Tsaybahe Group) with Middle Permian to Middle Triassic suprasubduction zone ophiolites in the Atlin terrane and interpreted them as constituent parts of an extensional arc system.

Further geochemical and geological investigation is needed to establish the significance of the Rosy Lake metagabbro, but the overlapping ages and lithological similarities raise a question as to whether and/or how this part of Yukon-Tanana interacted with the Middle

Triassic arc. The only other direct evidence for Middle Triassic magmatism in Yukon-Tanana is pegmatite from the Livingstone Creek area (Colpron *et al.* 2017). Gaidies *et al.* (2020) presented a Lu-Hf date of 245.3 ± 0.8 Ma from garnet within the Snowcap assemblage of western Yukon-Tanana terrane. The composition of the garnet core indicates that it grew during heating at low-pressure, but the cause of this heating is uncertain. One possibility is that Middle Triassic mafic magmatism affected other parts of Yukon Tanana and the low-pressure metamorphism documented by Gaidies *et al.*, (2020) is the result of contact metamorphism adjacent to an unrecognized intrusion.

Acknowledgements

Thanks to Kim Hatcher (2020) and Cassis Lindsay (2021) for their dedication and perseverance during field work, to Maurice Colpron for providing helpful feedback on an earlier version of the manuscript, and to Karen MacFarlane for technical editing and production.

References

Barresi, T., 2004. Sedimentology, structure, and depositional setting of the Loon Lake sedimentary rock unit, southern Semenof Hills, central Yukon. Unpublished BSc Honours thesis, Saint Mary's University, Halifax, Nova Scotia, 85 p.

Berman, R.G., Ryan, J.J., Gordey, S.P. and Villeneuve, M. 2007. Permian to Cretaceous polymetamorphic evolution of the Stewart River region, Yukon-Tanana terrane, Yukon, Canada: P-T evolution linked with in situ SHRIMP monazite geochronology. Journal of Metamorphic Geology, vol. 25, p. 803–827.

Bickerton, L., Colpron, M., Gibson, H.D., Thorkelson, D. and Crowley, J.L., 2020. The northern termination of the Cache Creek terrane in Yukon: Middle Triassic arc activity and Jurassic-Cretaceous structural imbrication. Canadian Journal of Earth Sciences, vol. 57, p. 227–248.

Bordet, E., Crowley, J.L. and Piercey, S.J., 2019. Geology of the eastern Lake Laberge area (105E), south-central Yukon. Yukon Geological Survey, Open File 2019-1, 120 p.

Brown, P. and Kahlert, B., 1986. Geology and mineralization of the Red Mountain porphyry molybdenum deposit south-central Yukon. *In*: Mineral deposits of Northern Cordillera, J.A. Morin (ed.), Canadian Institute of Mining and Metallurgy, Special Volume 37. p. 288–297.

Clarke, A.D., 2017. Tectonometamorphic history of mid-crustal rocks at Aishihik Lake, southwest Yukon. Unpublished MSc thesis, Simon Fraser University, Vancouver, British Columbia.

Cockfield, W.E., Lees, E.J. and Bostock, H.S. 1936. Laberge sheet, Yukon Territory. Geological Survey of Canada, "A" series map 372A, scale 1: 253,440.

Colpron, M., Murphy, D.C., Nelson, J.L., Roots, C.F., Gladwin, K., Gordey, S.P., Abbott, G. and Lipovsky, P., 2002. Preliminary geological map of Glenlyon (105L/1-7, 11-14) and northeast Carmacks (115I/9,16) areas, Yukon Territory (1:125 000 scale). Exploration and Geological Services Division, Yukon Region, Indian and Northern Affairs Canada, Open File 2002-9, also Geological Survey of Canada Open File 1457.

Colpron, M., Murphy, D.C., Nelson, J.L., Roots, C.F., Gladwin, K., Gordey, S.P. and Abbott, J.G., 2003. Yukon Targeted Geoscience Initiative, Part 1: Results of accelerated bedrock mapping in Glenlyon (105L/1-7, 11-14) and northeast Carmacks (115I/9,16) areas, central Yukon. *In:* Yukon Exploration and Geology 2002, D.S. Emond and L.L. Lewis (eds.), Exploration and Geological Services Division, Yukon Region, Indian and Northern Affairs Canada, p. 85–108.

Colpron, M., 2005a. Geological map of Livingstone Creek area (NTS 105E/8), Yukon (1:50 000 scale). Yukon Geological Survey, Open File 2005-9.

Colpron, M. 2005b. Preliminary investigation of the bedrock geology of the Livingstone Creek area (NTS 105E/8), south-central Yukon. *In:* Yukon Exploration and Geology 2004, D.S. Emond, L.L. Lewis and G.D. Bradshaw (eds.), Yukon Geological Survey, p. 95–107.

Colpron, M., 2006. Geology and mineral potential of Yukon-Tanana Terrane in the Livingstone Creek area (NTS 105E/8), south-central Yukon. *In:* Yukon Exploration and Geology 2005, D.S. Emond, G.D. Bradshaw, L.L. Lewis and L.H. Weston (eds.), Yukon Geological Survey, p. 93–107.

Colpron, M., Nelson, J.L. and Murphy, D.C., 2006a. A tectonostratigraphic framework for the pericratonic terranes of the northern Cordillera. *In:* Paleozoic Evolution and Metallogeny of Pericratonic Terranes at the Ancient Pacific Margin of North America, Canadian and Alaskan Cordillera, Colpron, M. and Nelson, J.L. (eds.), Geological Association of Canada, Special Paper 45, p. 1–23.

Colpron, M., Mortensen, J.K., Gehrels, G.E. and Villeneuve, M., 2006b. Basement complex, Carboniferous magmatism and Paleozoic deformation in Yukon-Tanana terrane of central Yukon: Field, geochemical and geochronological constraints from Glenlyon map area. *In:* Paleozoic Evolution and Metallogeny of Pericratonic Terranes at the Ancient Pacific Margin of North America, Canadian and Alaskan Cordillera, Colpron, M. and Nelson, J.L. (eds.), Geological Association of Canada, Special Paper 45, p. 131–151.

Colpron, M. and Nelson, J.L. 2011. A digital atlas of terranes for the Northern Cordillera. British Columbia Geological Survey and Yukon Geological Survey, 7 p.

Colpron, M., Israel, S., Murphy, D., Pigage, L. and Moynihan, D., 2016. Yukon bedrock geology map, 1:1 000 000. Yukon Geological Survey, Open File 2016-1.

Colpron, M., 2017. Revised geological map of Livingstone Creek area (NTS 105E/8), 1:50 000. Yukon Geological Survey, Open File 2017-1.

Colpron, M., Carr, S., Hildes, D. and Piercey, S., 2017. Geophysical, geochemical and geochronological constraints on the geology and mineral potential of the Livingstone Creek area, south-central Yukon (NTS 105E/8). *In:* Yukon Exploration and Geology 2016, K.E. MacFarlane and L.H. Weston (eds.), Yukon Geological Survey, p. 47–86.

Crowley, J.L., Schoene, B. and Bowring, S.A., 2007. U-Pb dating of zircon in the Bishop Tuff at the millennial scale. Geology, vol. 35, p. 1123–1126.

Gabrielse, H., Murphy, D.C. and Mortensen, J.K., 2006, Cretaceous and Cenozoic dextral orogen-parallel displacements, magmatism, and paleogeography, north-central Canadian Cordillera. *In:* Paleogeography of the North American Cordillera: Evidence For and Against Large-Scale Displacements, J.W. Haggart, R.J. Enkin and J.W.H. Monger (eds.), Geological Association of Canada, Special Paper 46, p. 255–276.

Gaidies, F., Morneau, Y.E., Petts, D.C., Jackson, S.E., Zagorevski, A. and Ryan, J., 2021. Major and trace element mapping of garnet: Unravelling the conditions, timing and rates of metamorphism of the Snowcap assemblage, west-central Yukon. Journal of Metamorphic Geology, 32 p., https://onlinelibrary.wiley.com/doi/10.1111/jmg.12562.

Gallagher, 1999. Regional-scale transposition and late large-scale folding in the Teslin Zone, Pelly Mountains, Yukon. Unpublished MSc thesis, Carleton University, Ottawa, Ontario, 199 p.

Gleeson, T.P., Friedman, R.M. and Wahl, K., 2000. Stratigraphy, structure, geochronology and provenance of the Logjam area, northwestern British Columbia (NTS 104O/14W). *In:* British Columbia Geological Survey, Geological Fieldwork 1999, Paper 2000-1, p. 297–306.

Gordey, S.P. and Makepeace, A.J., 2001. Bedrock Geology, Yukon Territory. Geological Survey of Canada, Open File 3754, scale 1:1 000 000.

Gordey, S.P. and Stevens, R.A., 1994. Preliminary interpretation of bedrock geology of the Teslin area (105C), southern Yukon. Geological Survey of Canada, Open File 2886 (1:250 000).

Gordey, S.P., McNicoll, V.J. and Mortensen, J.K., 1998. New U-Pb ages from the Teslin area, southern Yukon, and their bearing on terrane evolution in the northern Cordillera. *In:* Radiogenic age and isotopic studies, report 11. Geological Survey of Canada, Current Research 1998-F, p. 129–148.

Hansen, V.L., 1989. Structural and kinematic evolution of the Teslin suture zone, Yukon: record of an ancient transpressional margin. Journal of Structural Geology, vol. 11, p. 717–733.

Hansen, V.L., Mortensen, J.K. and Armstrong, R.L., 1989. U-Pb, Rb-Sr, and K-Ar isotopic constraints for ductile deformation and related metamorphism in the Teslin suture zone, Yukon Tanana terrane, south-central Yukon. Canadian Journal of Earth Sciences, vol. 26, p. 2224–2235.

Hansen, V.L., Heizler, M.T. and Harrison, T.M., 1991. Mesozoic thermal evolution of the Yukon-Tanana composite terrane: new evidence from $^{40}Ar/^{39}Ar$ data. Tectonics, vol. 10, p. 51–76.

Hansen, V.L., 1992. P-T evolution of the Teslin suture zone and Cassiar tectonites, Yukon, Canada: evidence for A- and B-type subduction. Journal of Metamorphic Geology, vol. 10, p. 239–263.

Hunt, P.A. and Roddick, J.C. 1992. A compliation of K-Ar and $^{40}Ar/^{39}Ar$ ages: report 22. *In:* Radiogenic Age and Isotopic studies: Report 6. Geological Survey of Canada, Paper 92-2, p. 179–226.

Harvey, J.L., Brown, R.L. and Carr, S.D., 1996. Progress in structural mapping in the Teslin suture zone, Big Salmon Range, central Yukon Territory. *In*: Slave-Northern Cordillera Lithospheric Evolution (SNORCLE) Transect and Cordilleran Tectonics Workshop Meeting, F. Cook and P. Erdmer (eds.), Lithoprobe Report No. 50, p. 33–34.

Harvey, J.L., Carr, S.D., Brown, R.L. and Gallagher, C., 1997. Deformation history and geochronology of plutonic rocks near the d'Abbadie fault, Big Salmon Range, Yukon. *In*: Slave-Northern Cordillera Lithospheric Evolution (SNORCLE) Transect and Cordilleran Tectonics Worksghop Meeting, F. Cook and P. Erdmer (eds.), Lithoprobe Report No. 56, p. 103–114.

Jaffey, A.H., Flynn, K.F., Glendenin, L.E., Bentley, W.C. and Essling, A.M., 1971. Precision measurements of half-lives and specific activities of ^{235}U and ^{238}U. Physical Review C, vol. 4, p. 1889–1906.

de Keijzer, M., Williams, P.F. and Brown, R.L., 1999. Kilometre-scale folding in the Teslin zone, northern Canadian Cordillera, and its tectonic implications for the accretion of the Yukon-Tanana terrane to North America. Canadian Journal of Earth Sciences, vol. 36, p. 479–494.

Kiss, F. and Boulanger, O., 2018. Residual Total Magnetic Field, Aeromagnetic Survey of the Marsh Lake Area, Yukon, Part of NTS 105F/North. Yukon Geological Survey, Open File 2018-17, also Geological Survey of Canada, Open File 8426, https://doi.org/10.4095/308237.

Lees, E.J., 1936. Geology of the Teslin-Quiet Lake area, Yukon. Geological Survey of Canada, Memoir 203, 30 p.

Mattinson, J.M., 2005. Zircon U-Pb chemical abrasion ("CA-TIMS") method: combined annealing and multi-step partial dissolution analysis for improved precision and accuracy of zircon ages. Chemical Geology, vol. 220, p. 47–66.

Mihalynuk, M.G., Friedman, R.M., Devine, F. and Heaman, L.M., 2006. Protolith age and deformation history of the Big Salmon Complex, relics of a Paleozoic continental arc in northern British Columbia. *In:* Paleozoic Evolution and Metallogeny of Pericratonic Terranes at the Ancient Pacific Margin of North America, Canadian and Alaskan Cordillera, M. Colpron and J.L. Nelson (eds.), Geological Association of Canada, Special Paper 45, p. 179–200.

Moynihan, D., 2022. Preliminary geological map of the Boswell River area (Parts of NTS 105C/13, 105C/14, 105F/4 and 105E/1). Yukon Geological Survey, Open File 2022-3, scale 1:50 000.

Mulligan, R. 1963. Geology of the Teslin map-area, Yukon Territory. Geological Survey of Canada, Memoir 326, 96 p.

Murphy, D.C., Mortensen, J.K., Piercey, S.J., Orchard, M.J. and Gehrels, G.E., 2006, Mid-Paleozoic to early Mesozoic tectonostratigraphic evolution of Yukon-Tanana and Slide Mountain terranes and affiliated overlap assemblages, Finlayson Lake massive sulphide district, southeastern Yukon. *In:* Paleozoic Evolution and Metallogeny of Pericratonic Terranes at the Ancient Pacific Margin of North America, Canadian and Alaskan Cordillera, M. Colpron and J.L. Nelson (eds.), Geological Association of Canada, Special Paper 45, p. 75–105.

Pattison, D.R.M, and Vogl, J.J., 2005. Contrasting sequences of metapelitic mineral-assemblages in the aureole of the tilted Nelson batholith, British Columbia: implications for phase equilibria and pressure determination in andalusite-sillimanite-type settings. The Canadian Mineralogist, vol. 43, p. 51–88.

Read, P.B., 1983. Geology, Classy Creek (104J/2E) and Stikine Canyon (104J/1W), British Columbia. Geological Survey of Canada, Open File 940, 1:50 000 scale.

Roots, C.F., Nelson, J.L., Simard, R.-L. and Harms, T.A., 2006. Continental fragments, mid-Paleozoic arcs and overlapping late Paleozoic arc and Triassic sedimentary strata in the Yukon-Tanana terrane of northern British Columbia and southern Yukon. *In:* Paleozoic Evolution and Metallogeny of Pericratonic Terranes at the Ancient Pacific Margin of North America, Canadian and Alaskan Cordillera, M. Colpron and J.L. Nelson (eds.), Geological Association of Canada, Special Paper 45, p. 153–177.

Sack, P.J, Colpron, M., Crowley, J., Ryan, J., Allan, M.M., Beranek, L.P. and Joyce, N.L., 2020. An atlas of Late Triassic to Jurassic plutons in the Intermontane terranes of Yukon. Yukon Geological Survey, Open File 2020-1.

Schmitz, M.D. and Schoene, B., 2007. Derivation of isotope ratios, errors and error correlations for U-Pb geochronology using ^{205}Pb-^{235}U-(^{233}U)-spiked isotope dilution thermal ionization mass spectrometric data. Geochemistry, Geophysics, Geosystems (G^3), vol. 8, Q08006, doi:10.1029/2006GC001492.

Simard, R.-L. 2003. Geological map of Southern Semenof Hills (part of NTS 105E/1,7,8), south-central Yukon (1:50 000 scale). Yukon Geological Survey, Open File 2003-12.

Simard, R.-L. and Devine, F., 2003. Preliminary geology of the southern Semenof Hills, central Yukon (105E/1,7,8). *In:* Yukon Exploration and Geology 2002, D.S. Emond and L.L. Lewis (eds.), Exploration and Geological Services Division, Yukon Region, Indian and Northern Affairs Canada, p. 213–222.

Simard, R.-L., Dostal, J. and Roots, C., 2003. Development of late Paleozoic volcanic arcs in the Canadian Cordillera: an example from the Klinkit Group, northern British Columbia and southern Yukon. Canadian Journal of Earth Sciences, vol. 40, p. 907–924.

Smith, J.L. and Arehart, G.B., 2010. Isotopic investigation of the Adanac porphyry molybdenum deposit in northwestern British Columbia (NTS 104N/11): final project report. *In:* Geoscience BC Summary of Activities 2009, Geoscience BC, Report 2010-1, p. 115–126.

Stevens, R.A., 1994. Structural and tectonic evolution of the Teslin tectonic zone, Yukon: a double vergent transpressive shear zone. Unpublished PhD thesis, University of Alberta, Edmonton, Alberta, 208 p.

Stevens, R.A., Erdmer, P., Creaser, R.A. and Grant, S.L., 1995. Mississippian assembly of the Nisutlin assemblage: evidence from primary contact relationships and Mississippian magmatism in the Teslin tectonic zone, part of the Yukon-Tanana terrane of south-central Yukon. Canadian Journal of Earth Sciences, vol 33, p. 103–116.

Stevens, R.D., Lachance, G.R. and DeLabio., 1982. Age determinations and geological studies K-Ar isotopic ages, report 16. Geological Survey of Canada, Paper 82-2, 56 p.

Taylor, B., 1975. Geological, geochemical and geophysical report on the SM claims, 41 p. Yukon Department of Energy, Mines and Resources, Assessment Report 090005.

Tempelman-Kluit, D.J., 1979. Transported cataclasite, ophiolite and granodiorite in the Yukon: evidence of arc-continent collision. Geological Survey of Canada, Paper 79-14, 27 p.

Tempelman-Kluit, D.J., 1984. Geology, Laberge and Carmacks, Yukon Territory. Geological Survey of Canada, Open File 1101, 10 p.

Tempelman-Kluit, D.J., 2009. Geology of Carmacks and Laberge map areas, central Yukon: Incomplete draft manuscript on stratigraphy, structure and its early interpretation (*ca.* 1986). Geological Survey of Canada, Open File 5982, 399 p.

Westberg, 2010. The tectonometamorphic and structural evolution of the Yukon-Tanana and Cassiar terranes in the Mendocina Creek area: implications for the tectonic framework of south-central Yukon. Unpublished MSc thesis, Simon Fraser University, Vancouver, British Columbia.

van Straaten, B.I. and Wearmouth, C., 2019. Geology of the Latham and Pallen Creek area, northwestern British Columbia: Distinguishing the Tsaybahe group, Stuhini Group, and Hazelton Group, and the onset of Triassic arc volcanism in northern Stikinia. *In:* Geological Fieldwork 2018, British Columbia Ministry of Energy, Mines and Petroleum Resources, British Columbia Geological Survey, Paper 2019-01, p. 79–96.

Yukon Geological Survey, 2021. Yukon Geochronology – A database of Yukon isotopic age determinations. Yukon Geological Survey, http://data.geology.gov.yk.ca/Compilation/22, [accessed December, 2021].

Zagorevski, A., van Staal, C.R., Bedard, J.H., Bogatu, A., Canil, D., Coleman, M., Golding, M., Joyce, N.L., Lawley, C., McGoldrick, S., Mihalynuk, M.G., Milidragovic, D., Parson, A., Schiarizza, P., 2021. *In:* Northern Cordillera geology: a synthesis of research from the Geo-mapping for Energy and Minerals program, British Columbia and Yukon, J.J. Ryan and A. Zagorevski (eds.), Geological Survey of Canada, Bulletin 610, p. 21–65.

Appendix

The appendix includes three folders—CL zircon images, LA-ICPMS_tables, and U-Pb geochronology methods—and is only available digitally. The .zip file that accompanies this document and can be downloaded from https://data.geology.gov.yk.ca.